Modelling Electricity Prices: A Time Change Approach

Lingfei Li* Rafael Mendoza-Arriaga† Zhiyu Mo‡ Daniel Mitchell§

February 16, 2016

Abstract

To capture mean reversion and sharp seasonal spikes observed in electricity prices, this paper develops a new stochastic model for electricity spot prices by time changing the Jump Cox-Ingersoll-Ross (JCIR) process with a random clock that is a composite of a Gamma subordinator and a deterministic clock with seasonal activity rate. The time-changed JCIR process is a time-inhomogeneous Markov semimartingale which can be either a jump-diffusion or a pure-jump process, and it has a mean-reverting jump component that leads to mean reversion in the prices in addition to the smooth mean-reversion force. Furthermore, the characteristics of the time-changed JCIR process are seasonal, allowing spikes to occur in a seasonal pattern. The Laplace transform of the time-changed JCIR process can be efficiently computed by Gauss-Laguerre quadrature. This allows us to recover its transition density through efficient Laplace inversion and to calibrate our model using maximum likelihood estimation. To price electricity derivatives, we introduce a class of measure changes that transforms one time-changed JCIR process into another time-changed JCIR process. We derive a closed-form formula for the futures price and obtain the Laplace transform of futures option price in terms of the Laplace transform of the time-changed JCIR process, which can then be efficiently inverted to yield the option price. By fitting our model to two major electricity markets in the US, we show that it is able to capture both the trajectorial and the statistical properties of electricity prices. Comparison with a popular jump-diffusion model is also provided.

Keywords: electricity spot prices, electricity futures and futures options, spikes, mean-reversion, seasonality, stochastic time change, Laplace transform.

JEL Classification: G12, G13.

1 Introduction

The deregulation of electricity markets in many countries has drastically changed the behavior of electricity prices, which are now determined according to the fundamental law of demand and

*Department of Systems Engineering and Engineering Management, The Chinese University of Hong Kong. Email: lfli@se.cuhk.edu.hk.

†Department of Information, Risk and Operations Management, McCombs School of Business, The University of Texas at Austin. Email: rafael.mendoza-arriaga@mccombs.utexas.edu.

‡Department of Systems Engineering and Engineering Management, The Chinese University of Hong Kong. Email: zymo@se.cuhk.edu.hk.

§Engineering System and Design, Singapore University of Technology and Design. Email: daniel_mitchell@sutd.edu.sg.

supply. In practice, electricity prices are extremely volatile, with annualized volatility typically being *several hundred percent* (Eydeland and Wolyniec (2003), p.86), which is a level that has never been observed for any other financial asset or commodity. A stochastic model that captures the peculiar behavior of electricity prices is therefore necessary and crucial for risk management, derivative pricing and operational decisions in electricity markets.

In this paper, we are concerned with modelling electricity spot prices and pricing electricity derivatives including futures and futures options based on the spot model. Electricity markets are different from other commodity markets for both spot and futures. For electricity, a large part of the spot trading is organized in the day-ahead market. On each day, the price for every hour in the following day is determined by the aggregate supply and demand for that hour. The day-ahead average price is calculated by averaging twenty-four hourly prices, and it is used as the reference price in many financially settled futures contracts. For these reasons, the literature often regards the day-ahead average price as the spot price (see, e.g., Lucia and Schwartz (2002)). In this paper we model the day-ahead average price and follow the convention to call it as the spot price. In the futures market, unlike other commodities, electricity futures require delivery over a time period which is typically a month, a quarter or a year, rather than at a fixed time. This special feature imposes restrictions on the spot model if one wants to obtain tractability for pricing futures and futures options, which is a very important consideration in practice.

Electricity prices display two salient features in their sample paths. First, similar to many other commodities, they are reverting to a mean level. Depending on the market, this level can display weekly, quarterly or annual seasonality. Second, unlike other commodities, electricity prices exhibit very sharp spikes, which are large upward moves followed shortly by steep downward moves towards a normal price range. Due to the inelastic demand, the exponentially increasing supply function, and the non-storable nature of electricity, power prices can easily jump by orders of magnitude, for instance from \$40/MWH to \$120/MWH, as a result of demand and supply shocks caused by, e.g., extreme weather conditions, plant outages and transmission disruptions (Geman (2005)). These shocks usually last for a short time, causing the price to quickly fall back to the normal level, and hence, creating sharp spikes in the price trajectory. A further feature of spikes is that in some markets they are concentrated in summer and/or winter.

Let $(S_t)_{t\geq 0}$ denote the electricity spot price process. In the literature, the spot price is often modeled as

$$S_t = \Lambda(t)X_t,$$

where $\Lambda(t)$ is a deterministic function that models the seasonal trend to which the price reverts, and X_t is a stochastic process to model the random fluctuations from the trend. In the literature, X_t is also known as the *deseasonalized spot price*, i.e., the price after removing the seasonal trend. We observe, however, that even after factoring out $\Lambda(t)$, the behavior of X_t may still exhibit some seasonal behavior, e.g., the arrival rate of spikes, as well as the volatility level, tend to increase during peak seasons. The challenge lies in specifying X_t so that the model is not only able to capture trajectorial as well as statistical features of electricity prices, but also computationally tractable for calibration and pricing purposes.

There are already many models for X_t. As an extension to the classical commodity model of Schwartz (1997), which is based on the Ornstein-Uhlenbeck (OU) diffusion, some authors (e.g., Cartea and Figueroa (2005), Kjaer (2008), Weron (2008)) propose to model $\ln X_t$ by a Markovian mean-reverting jump diffusion, where the diffusion part is specified as OU, and jumps are modeled

by a compound Poisson process that is independent of the diffusion part. By specifying the jump size to follow the normal distribution, Cartea and Figueroa (2005) obtained an analytical formula for the futures price, but pricing futures options is not tractable. A common drawback of this type of models is that they require a high level of mean-reversion speed to generate spikes, because mean-reversion is only realized through the diffusion drift. Consequently, normal price variations may be smoothed out. This issue motivated Geman and Roncoroni (2006) to introduce state-dependent jumps in the mean-reverting jump-diffusion process, where the direction of the jump depends on the relation between the pre-jump price and some threshold. If the price is below the threshold, then the next jump will be upward, otherwise downward. In this model, mean reversion to the normal price range is not only generated by the smooth mean-reversion force from the drift, but also by downward jumps. A potential problem with the threshold specification is that upward jumps are impossible when the price exceeds the threshold. Nonetheless, it is sometimes observed in the market that the spot price jumps up even when it is already very high. To estimate their model, Geman and Roncoroni (2006) develop an iterative procedure and show that it provides a good fit to the data from major US power markets. However, pricing electricity futures and options is not tractable in their model. To price such contracts, methods based on trees and numerically solving PIDEs are developed by Geman and Kourouvakalis (2008) and Albanese et al. (2012). Other ideas to model electricity spot prices include multi-factor models as in, e.g., Burger et al. (2004), Benth et al. (2007), Cartea and Villaplana (2008), Meyer-Brandis and Tankov (2008), Hambly et al. (2009), Birge et al. (2010), Klüppelberg et al. (2010), Jaimungal and Surkov (2011), Hayfavi and Talasli (2014) and Veraart and Veraart (2014); regime switching models as in, e.g., Deng (1999), Huisman and Mahieu (2001), Weron et al. (2004) and Nomikos and Soldatos (2008); and time-series models based on autoregressive and GARCH specifications as in e.g., Escribano et al. (2011).

In this paper, we aim to develop a new stochastic model for electricity spot prices within the one-dimensional Markovian framework in view of the fact that models based on one-dimensional Markov processes are often more tractable, and they require less computational effort in pricing derivatives, especially exotic ones. In particular, we want our stochastic model to exhibit jumps that contribute to mean-reversion, and it should be able to capture the trajectorial as well as the statistical properties of electricity prices (that is, we want our model to reproduce mean reversion and seasonal spikes, and also provide a good match of the moments, including skewness and kurtosis). Moreover, the model should be tractable for pricing futures and futures options. To construct a jump process model with the required features, we employ the method of random time changes. The typical approach used in the literature for constructing a Markovian jump process Y via time changes starts with a time-homogeneous diffusion process X that is subsequently time changed with an independent Lévy subordinator L (a nonnegative Lévy process), i.e., $Y_t = X_{L_t}$, for $t \geq 0$. The resulting process Y is often called a subordinate diffusion. Y is a time-homogeneous Markov process due to the independent and stationary increments of L, and it can be either a jump-diffusion or a pure-jump process, depending on whether the drift of L is positive or zero. When the jumps of L have infinite (resp., finite) activity, the jumps of Y have infinite (resp., finite) activity as well. If X is a Brownian motion, Y is a Lévy process whose jumps are state-independent. But more generally, the jumps of Y are state-dependent. For instance, if X is a mean-reverting diffusion, then the jumps of Y are also mean-reverting (see Li and Linetsky (2014) for an example). Applications of Lévy subordination of diffusions in equity, credit, interest rate and commodity markets can be found in e.g. Madan et al. (1998), Barndorff-Nielsen (1998), Madan and Yor (2008), Boyarchenko and Levendorskiĭ (2007), Mendoza-Arriaga et al. (2010), Lim et al. (2012), Mendoza-Arriaga and

Linetsky (2013) and Li and Linetsky (2014). Unfortunately, subordinate diffusions are not quite appropriate for modelling electricity prices. For instance, although subordinate diffusions exhibit jumps, the probability of having extremely large jumps like a jump from \$40/MWH to \$120/MWH is very small. Moreover, subordinate diffusions have time-homogeneous characteristics, which do not match the seasonal volatility and jumps that are typically observed in electricity markets.

Therefore, in order to develop a time-changed process with the desirable features, we must use different specifications for the background process and the time change from those used in the literature. To produce upward jumps with large magnitude and to obtain tractability, we choose the Cox-Ingersoll-Ross (CIR) diffusion interspersed with compound Poisson jumps with exponentially distributed jump size as our background process X (see Eq. (2)). This process is often known as the *Basic Affine Jump-Diffusion* in the literature (Duffie and Gârleanu (2001)), but hereafter we call it *Jump-CIR (JCIR)* process. To create seasonal spikes, we set the random clock T to be defined as $T_t = L_{A_t}$, where L is a Gamma process (a popular Lévy subordinator used in finance) and $A_t = \int_0^t a(u)du$ with the activity rate $a(u)$ being a deterministic seasonal function of time. Then, the deseasonalized spot price process is modelled by the time-changed JCIR process X_{T_t}, which is a time-inhomogeneous Markov process, and it can be specified either as a jump-diffusion ($\gamma > 0$) or as a pure-jump process ($\gamma = 0$), where γ is the drift of the Gamma subordinator (see Eq. (3)). Our model exhibits two notable features in its sample paths. *First*, in contrast to the JCIR process, which can only jump upward with jumps being state-independent, the jump measure of the time-changed JCIR process has a state-dependent and mean-reverting component which allows both upward and downward jumps. Thus in our model, mean reversion can be realized via jumps as well as continuous drift. In the pure-jump specification, the diffusion drift term vanishes, and hence, mean reversion is solely carried out by jumps. Compared to the threshold specification of Geman and Roncoroni (2006), our model does not rule out the possibility of upward jumps at high spot prices. *Second*, in our model the diffusion drift, volatility, and jump measure are all time dependent and seasonal. To be more specific, during seasons like summer and winter when demand and supply shocks are more likely to occur, the diffusion volatility and upward jump intensity become stronger, meanwhile the smooth mean-reversion force and downward jump intensity also strengthen. Therefore, during these seasons, any large price deviations from the mean level will be pulled back quickly, resulting in more spikes compared to other seasons.

The time-changed JCIR process is computationally tractable. Its Laplace transform can be computed efficiently through Gauss-Laguerre quadrature. From the Laplace transform, one can recover the transition density of the time-changed JCIR process via an efficient Laplace inversion algorithm, such as the one by Abate and Whitt (1992). This allows us to estimate our model using maximum likelihood estimation.

To price electricity derivatives, we develop a class of equivalent measure changes that transforms one time-changed JCIR process into another time-changed JCIR process. Using these measure transformations, our model remains in the same form under the pricing measure so that derivative pricing is also tractable. We obtain a simple closed-form formula for the futures price as well as the Laplace transform of the futures option price, which can then be efficiently inverted to yield the option price. To price popular exotic options like swing options, one can apply the efficient Fourier-cosine expansion method of Zhang and Oosterlee (2013).

We provide a detailed mathematical analysis of the time-changed JCIR process in this paper. We characterize it as a time-inhomogeneous Markov semimartingale and obtain its family of generators as well as semimartingale characteristics. These results allow us to obtain insights into the

trajectorial features of our model, and they are also the basis for developing equivalent measure changes. Our analysis is built upon the recent theory of additive subordination developed in Li et al. (2015) by recognizing that the time change we use is a special type of additive subordinators, which are nonnegative and nondecreasing additive processes. However, there are several places where the analysis of the time-changed JCIR process requires arguments that are different from those used in the analysis of additive subordinate diffusions in Li et al. (2015).

The rest of the paper is organized as follows. Section 2 describes the modelling framework. Section 3 provides a detailed mathematical analysis of time-changed JCIR processes. In this section, we go beyond the Gamma process to consider general Lévy subordinators as the theoretical results hold generally. In Section 4, we first study equivalent measure changes for time-changed JCIR processes and then price electricity futures and futures options. Section 5 shows how to estimate the model and provides calibration examples to two major electricity markets in the US. The results show that our model provides a good fit both trajectorially and statistically. We also compare our model with the popular model of Cartea and Figueroa (2005) in terms of moment matching and price prediction. Section 6 concludes the paper. The appendix contains the exact simulation scheme for the time-changed JCIR process and proofs.

2 The Model Set-Up

We model the spot price as

$$S_t = \Lambda(t) X_t^{\phi},$$

where $\Lambda(t)$ is a deterministic function of time that models the trend, and X^{ϕ} is a positive stochastic process that models random fluctuations from the trend. We set $\Lambda(t)$ to be a parametric function of the form

$$\ln \Lambda(t) = a_0 + b_0 t + \sum_{i=1}^{n} a_i \cos(2\pi f_i t + b_i), \quad f_i > 0. \tag{1}$$

Observe that the trend function $\Lambda(t)$ includes the possibility for multiple seasonal behaviors that can occur at different frequencies, e.g., annual, semi-annual, quarterly, etc. Similar forms for the trend function are used in Geman and Roncoroni (2006), Meyer-Brandis and Tankov (2008) and Benth et al. (2012). We find that Eq.(1) is appropriate for the US markets we consider.

We model $(X_t^{\phi})_{t\geq 0}$ as a time-changed JCIR process, i.e., $X_t^{\phi} = X_{T_t}$, where X is a JCIR process and T is a random clock. A JCIR process is the unique solution to the following SDE:

$$dX_t = \kappa(1 - X_t)dt + \sigma\sqrt{X_t}dB_t + dJ_t, \;\; X_0 = x_0 > 0, \tag{2}$$

where $\kappa, \sigma > 0$ and J is a compound Poison process with arrival rate $\varpi > 0$ and the jump size follows an exponential distribution with mean $\mu > 0$. We set the mean level of X to be 1 since $\Lambda(t)$ is the trend to which S_t reverts. We also impose the Feller condition $2\kappa \geq \sigma^2$ so that zero is an unattainable boundary for X (see Cheridito et al. (2005), p.1727). The JCIR process is a suitable candidate for the background process, since its drift term exhibits mean-reversion and the compound Poisson part can generate large upward jumps. Furthermore, the JCIR's Laplace transform has a simple closed-form expression, which is important for obtaining tractability for X^{ϕ}.

We choose T_t to be in the form $T_t = L_{A_t}$. Here L is a Gamma process (see Madan et al. (1998)). Its Lévy measure is given by

$$\nu(d\tau) = \frac{m^2/v}{\tau} e^{-\frac{m}{v}\tau} d\tau,$$

where $m = \mathbb{E}[L_1] - \gamma$ and $v = \mathrm{Var}[L_1]$ are the mean and variance rate of the stochastic part of the Gamma process respectively and $\gamma \geq 0$ is the drift of L. The Laplace transform of the Gamma process is given by

$$\mathbb{E}[e^{-\lambda L_t}] = e^{-\psi(\lambda)t},$$

with the Laplace exponent

$$\psi(\lambda) = \gamma\lambda + \frac{m^2}{\nu} \ln\left(1 + \frac{\lambda\nu}{m}\right). \tag{3}$$

We further assume that L is independent of X. A_t is a deterministic and absolutely continuous function of time which is written as $A_t = \int_0^t a(u)du$, where $a(u)$ is interpreted as the activity rate. To model the phenomenon that spikes concentrate in winter and/or summer, we choose the activity rate $a(u)$ to be a positive bimodal periodic function with one-year period, depicted in Figure 1. The function is only plotted for one year, and it is extended to other times using periodicity. We choose the peak time t_{p1} to be in winter and t_{p2} to be in summer, and τ_1 (resp., τ_2) is the half length of the spike concentration period in winter (resp., summer). The value of $a(u)$ is normalized to one in periods outside winter and summer, and $1 + c_1$ (resp., $1 + c_2$) gives the maximum activity rate in winter (resp., summer). If spikes only concentrate in one of these seasons, then we set $c_1 = 0$ or $c_2 = 0$ accordingly. Under our specification, the integral $\int_s^t a(u)du$ can be easily computed in closed-form. We remark that, any other specification with similar shape can be used for $a(u)$, as long as $\int_s^t a(u)du$ is easy to compute.

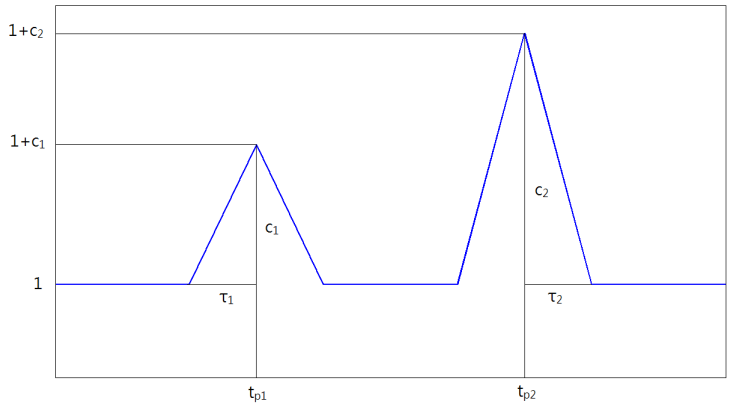

Figure 1: Activity rate $a(u)$ in a one-year period

From $T_t = L_{A_t}$, it is easy to see that T is an additive subordinator, i.e., a nonnegative and nondecreasing additive process (Sato (1999)). We refer readers to Li et al. (2015) for detailed discussions on general additive subordinators. In our case, the Laplace transform of T is given by

$(0 \le s < t)$

$$\mathbb{E}[e^{-\lambda(T_t - T_s)}] = e^{-\int_s^t \phi(\lambda,u)du} = e^{-\psi(\lambda)\int_s^t a(u)du},\ \phi(\lambda,u) = \gamma a(u)\lambda + \int_{(0,\infty)} \left(1 - e^{-\lambda\tau}\right) a(u)\nu(d\tau),$$

where $\phi(\lambda, \cdot)$ is called the density of the Laplace exponent, which explains why we use X_t^ϕ as the notation for X_{T_t}.

Under our modelling framework, other Lévy subordinators can also be used together with A_t to time change the JCIR process. The resulting models are able to produce similar trajectorial features as the model obtained from Gamma subordination. However, using the Gamma process we obtain a model that is most tractable for calibration and derivatives valuation (see Remark 2).

3 Time-Changed JCIR Processes

We call X^ϕ defined in Section 2 as the Lévy-AC time-changed JCIR process or LAC-JCIR for short if a general Lévy subordinator is used. In the case where the Gamma process is used, we call X^ϕ as the GMAC-JCIR process. In Section 3.1, we provide a detailed mathematical analysis of the LAC-JCIR process and results for the GMAC-JCIR process follow as a special case. The Markov and semimartingale characterization of the LAC-JCIR process help us understand the effect of time change and gain insights into the trajectories that can be generated by our model. The semimartingale characterization is also the basis for studying equivalent measure changes. In Section 3.2, we calculate the Laplace transform of the GMAC-JCIR process.

3.1 Markov and Semimartingale Characterization

We characterize the LAC-JCIR process as a time-inhomogeneous Markov semimartingale based on the general theory of additive subordination developed by Li et al. (2015). In general, the method of time changing a Markov process with an independent additive subordinator is called additive subordination. A LAC-JCIR process can be viewed as being obtained by applying additive subordination to a JCIR process with the additive subordinator obtained from time changing a Lévy subordinator by a deterministic absolutely continuous process.

Let $I = (0, \infty)$. We first point out some useful properties of the JCIR process X (see Eq. (2)). We denote its transition operator by $\mathcal{P}_t$ and its infinitesimal generator by $\mathcal{G}$. Since X is a regular affine process, from Theorem 2.7 in Duffie et al. (2003), X is a Feller-Dynkin process, i.e., $(\mathcal{P}_t)_{t\ge 0}$ is a strongly continuous semigroup of positivity-preserving contractions on $C_0([0,\infty))$ (the space of continuous functions on I vanishing at infinity), $C_c^2(I) \subset \mathrm{Dom}(\mathcal{G})$ ($C_c^2(I)$ is the space of twice continuously differentiable functions with compact support in I), and for all $f \in C_c^2(I)$ we have:

$$\mathcal{G}f(x) = \frac{1}{2}\sigma^2 x f''(x) + \kappa(1-x)f'(x) + \frac{\varpi}{\mu}\int_{(0,\infty)} (f(x+y) - f(x))e^{-\frac{y}{\mu}}dy. \tag{4}$$

We next present a precise mathematical framework for the LAC-JCIR process. We assume on a probability space $(\Omega, \mathbb{P})$, we have a JCIR process X satisfying (2) and an independent Lévy subordinator L with drift $\gamma \ge 0$ and Lévy measure ν satisfying $\int_{(0,\infty)}(s \wedge 1)\nu(ds) < \infty$. Both X and L have càdlàg sample paths. We refer readers to, for example, Song and Vondraček (2008) for the construction of such Ω and $\mathbb{P}$. We let $T_t(\omega) := L_{A_t}(\omega)$ and define $X_t^\phi(\omega) := X_{T_t(\omega)}(\omega)$, whose sample paths are also càdlàg, and we call $(\kappa, \sigma, \varpi, \mu, \gamma, \nu(\cdot), a(\cdot))$ the generating tuple of X^ϕ.

Letting $\mathcal{F}_t^0 = \sigma(X_u^\phi : 0 \le u \le t)$ to be the natural filtration generated by X^ϕ, X^ϕ is a Markov process with respect to $(\mathcal{F}_t^0)_{t\ge 0}$ due to the independent increments of T. In the following, in order to use results from Jacod and Shiryaev (2003), we will work with $\mathcal{F}_t := \mathcal{F}_{t+}^0 = \bigcap_{\tau>t} \mathcal{F}_\tau^0$, the right-continuous extension of the natural filtration. It turns out that X^ϕ is also Markov w.r.t. $(\mathcal{F}_t)_{t\ge 0}$, which we explain below.

Let us recall several notions first. A two-parameter family of operators $(Q_{s,t})_{0\le s\le t}$ on a Banach space $\mathfrak{B}$ is called a backward propagator if it satisfies (i) $Q(s,t) = Q(s,u)Q(u,t)$ for $0 \le s \le u \le t$; (ii) $Q(t,t) = I$ for $t \ge 0$. Backward propagator generalizes the notion of semigroup to the time dependent case. A backward propagator $(Q_{s,t})_{0\le s\le t}$ is called strongly continuous if for every $f \in \mathfrak{B}$, $(s,t) \mapsto Q_{s,t}f$ is continuous ($0 \le s \le t < \infty$). $Q_{s,t}$ is called a contraction if $\|Q_{s,t}f\| \le \|f\|$ for every $f \in \mathfrak{B}$. Define $\mathcal{G}_t f = \lim_{h\to 0+} \frac{Q_{t,t+h}f - f}{h}$. The domain of $\mathcal{G}_t$ consists of $f \in \mathfrak{B}$ such that the limit exists. We call $(\mathcal{G}_t)_{t\ge 0}$ the family of infinitesimal generators of the backward propagator $(Q_{s,t})_{0\le s\le t}$.

Let $q_{s,t}$ denote the distribution of $T_t - T_s$. From the time-change construction for X^ϕ, the backward propagator associated with X^ϕ, denoted by $(\mathcal{P}_{s,t}^\phi)_{0\le s\le t}$, is given by

$$\mathcal{P}_{s,t}^\phi f(x) := \int_{[0,\infty)} \mathcal{P}_u f(x) q_{s,t}(du), \ \ f \in C_0([0,\infty)). \tag{5}$$

Applying Theorem 3.1 in Li et al. (2015), $(\mathcal{P}_{s,t}^\phi)_{0\le s\le t}$ is a strongly continuous backward propagator of positivity-preserving contractions on $C_0([0,\infty))$, i.e., it is Feller-Dynkin (c.f. Gulisashvili and Van Casteren (2006), Definition 2.5). Hence, from Theorem 2.13 in Gulisashvili and Van Casteren (2006), X^ϕ is a Markov process with respect to $(\mathcal{F}_t)_{t\ge 0}$.

Denote the family of infinitesimal generators for X^ϕ by $(\mathcal{G}_t^\phi)_{t\ge 0}$. Li et al. (2015) derived a relation between $\mathcal{G}_t^\phi$ and $\mathcal{G}$ under general additive subordination. Based on this relation, the next proposition presents an explicit expression for $\mathcal{G}_t^\phi$. In the following, $p(\tau,x,y)$ denotes the transition probability density of the JCIR process, and for notational simplicity, we extend $p(\tau,x,y)$ for y from I to $\mathbb{R}$ by defining $p(\tau,x,y) = 0$ for $y \notin I$.

Proposition 1. *For $f \in C_c^2(I)$,*

$$\begin{aligned}\mathcal{G}_t^\phi f(x) &= \frac{1}{2}(\sigma^\phi(t,x))^2 f''(x) + \mu^\phi(t,x) f'(x) \\ &\quad + \int_{y\ne 0} \left(f(x+y) - f(x) - 1_{\{|y|\le 1\}} y f'(x)\right) \left(1_{\{y>0\}} \gamma a(t) \frac{\varpi}{\mu} e^{-\frac{y}{\mu}} dy + \Pi^\phi(t,x,dy)\right)\end{aligned}$$

where for $t \ge 0$,

$$\begin{aligned}\mu^\phi(t,x) &= \gamma a(t)[\kappa(1-x) + \varpi(1 - e^{-\frac{1}{\mu}})] + a(t) \int_{(0,\infty)} \int_{\{|y|\le 1\}} y p(\tau,x,x+y) dy \nu(d\tau), \\ \sigma^\phi(t,x) &= \sigma\sqrt{\gamma a(t) x}, \\ \Pi^\phi(t,x,dy) &= \pi^\phi(t,x,y)dy, \quad \pi^\phi(t,x,y) = a(t) \int_{(0,\infty)} p(\tau,x,x+y)\nu(d\tau), \ \text{for } y \ne 0.\end{aligned} \tag{6}$$

$\Pi^\phi(t,x,dy)$ is a Levy-type measure, i.e. $\int_{y\ne 0}(1 \wedge y^2)\Pi^\phi(t,x,dy) < \infty$.

We define $\pi^0(t,y) := 1_{\{y>0\}}\gamma a(t)\frac{\varpi}{\mu}e^{-\frac{y}{\mu}}$, and

$$\widehat{\pi}^{\phi}(t,x,y) := \pi^0(t,y) + \pi^{\phi}(t,x,y),\ \widehat{\Pi}^{\phi}(t,x,dy) := \widehat{\pi}^{\phi}(t,x,y)dy. \tag{7}$$

Then $\widehat{\Pi}^{\phi}(t,x,dy)$ is the jump measure in the generator, which is both time and state dependent. It consists of two parts. The first part is the JCIR jump measure scaled by $\gamma a(t)$, which has finite activity and it is concentrated on $y>0$. The second part, $\Pi^{\phi}(t,x,dy)$, is generated by time change, which places non-zero measure on both $y>0$ and $y<0$. Using the definition of $\Pi^{\phi}(t,x,dy)$, it is easy to see that

$$\int_{y\neq 0}\Pi^{\phi}(t,x,dy) = a(t)\int_{(0,\infty)}\nu(d\tau).$$

Therefore $\Pi^{\phi}(t,x,dy)$ (and hence $\widehat{\Pi}^{\phi}(t,x,dy)$) has infinite activity if and only if the Lévy subordinator has infinite activity. We further observe that $\Pi^{\phi}(t,x,dy)$ is a state-dependent measure that exhibits *mean-reverting* effect due to mean-reversion in the JCIR process, i.e., when the current state is above (below) the long-run level, downward (upward) jumps are more likely to occur. In Figure 2, we plot the jump density $\pi^{\phi}(t,x,y)$ for different values of x using the Gamma subordinator while fixing the activity rate $a(t)$=1. We compute the density value by numerically integrating (6), where the transition density of the JCIR process $p(\tau,x,x+y)$ is obtained from Laplace inversion (the Laplace transform of the JCIR process is known in closed-form). To emphasize the value of the current state, the horizontal axis plots the post jump state, not the jump size. Recall that the mean-level is 1. The vertical line marks the current state value. It is clear from the graphs that when $x<1$, the area of the graph on the right of the current state is greater than the area on the left, i.e. upward jumps are more likely than downward jumps. When $x>1$, the reverse is observed, and as x increases, downward (upward) jumps become more (less) likely to occur (compare the left (right) tail of the graph for $x=2$ and $x=3.5$). Hence, when the spot price exceeds the mean-level by a significant amount, one can expect a downward jump to occur next with very high probability.

Based on the Markov characterization, the next proposition shows that X^{ϕ} is also a semimartingale and finds out its semimartingale characteristics and sample path decomposition (see Jacod and Shiryaev (2003) Chapter I and II for the definition of related concepts).

Proposition 2. *The LAC-JCIR process X^{ϕ} is a semimartingale on $(\Omega,(\mathcal{F}_t)_{t\geq 0},\mathbb{P})$, which admits the following semimartingale characteristics w.r.t. the truncation function $h(x)=x1_{\{|x|\leq 1\}}$,*

$$\begin{aligned} B_t^{\phi}(\omega) &= \int_0^t \Big[\gamma a(s)\kappa(1-X_{s-}^{\phi}(\omega)) + \gamma a(s)\varpi(1-e^{-\frac{1}{\mu}}) \\ &+ a(s)\int_{(0,\infty)}\int_{\{|y|\leq 1\}} yp(\tau,X_{s-}^{\phi}(\omega),X_{s-}^{\phi}(\omega)+y)dy\nu(d\tau)\Big]ds, \end{aligned} \tag{8}$$

$$C_t^{\phi}(\omega) = \int_0^t \gamma a(s)X_{s-}^{\phi}(\omega)\sigma^2 ds, \tag{9}$$

$$\nu^{\phi}(\omega,dt,dy) = \widehat{\pi}^{\phi}(t,X_{t-}^{\phi}(\omega),y)dydt. \tag{10}$$

where $\widehat{\pi}^{\phi}(t,x,y)$ is defined in (7). Denote by $X^{\phi,c}$ the continuous local martingale part of X^{ϕ} and J^{ϕ} the integer-valued random measure associated with the jumps of X^{ϕ}. ν^{ϕ} is the predictable compensator of J^{ϕ}. X^{ϕ} has the following sample path decomposition ($*$ denotes integration w.r.t. a random measure)

$$X_t^{\phi}(\omega) = x_0 + B_t(\omega) + X_t^{\phi,c}(\omega) + h(x)*(J^{\phi}-\nu^{\phi})_t(\omega) + (x-h(x))*J_t^{\phi}(\omega),$$

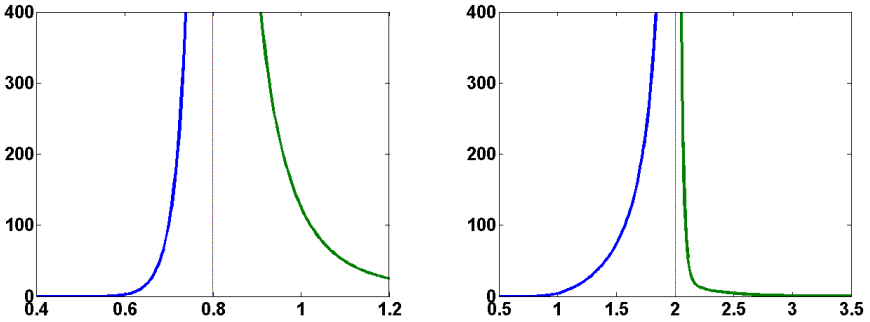

(a) $x = 0.8$ (b) $x = 2$

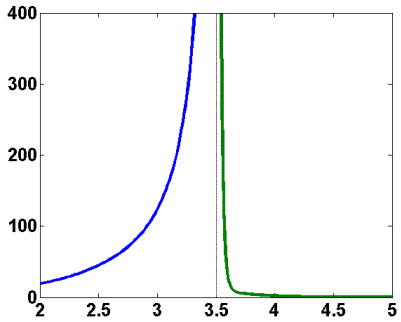

(c) $x = 3.5$

Figure 2: The value of the jump density $\pi^{\phi}(t, x, y)$ for the GMAC-JCIR process, where x is the current state and y is the post-jump state. The horizontal axis plots the post-jump state.

with the quadratic variation $[X^{\phi,c}, X^{\phi,c}]_t(\omega) = C_t(\omega)$.

From Proposition 1 and 2, we observe that X^{ϕ} is a time-inhomogeneous Markov semimartingale. Moreover, we observe that time change produces the following notable features in our model.

- **Jump-diffusion or pure-jump specification**: In the LAC-JCIR process, the drift, diffusion coefficient and jump measure of the JCIR process are all scaled by γ, the drift of the Lévy subordinator. From (9), if $\gamma = 0$, then the diffusion component vanishes and X^{ϕ} becomes a pure jump process, otherwise it is a jump-diffusion.

- **Mean-reverting jumps**: The Lévy measure of the Lévy subordinator introduces $\pi^{\phi}(t, x, y)$, a state-dependent component in the jump measure of the LAC-JCIR process, which allows for both upward and downward jumps and exhibits mean-reversion. Now there are two ways in which X^{ϕ} can return to the normal range after large upward jumps have occurred (and hence, producing sharp spikes). It can be realized either by mean-reverting jumps, or by the mean-reverting drift $\mu^{\phi}(t, x)$ which continuously pulls the process to the mean level. Furthermore, when $\gamma = 0$, i.e., in the pure-jump specification, the mean-reverting part of $\mu^{\phi}(t, x)$ vanishes and mean-reversion is solely carried out by jumps. We further remark that, in this case, although $\pi^{0}(t, y)$ disappears, large upward jumps can still be generated by $\pi^{\phi}(t, x, y)$ due to the JCIR's transition density $p(t, x, y)$ in Eq.(6) (see Figure 2 for an illustration).

- **Seasonal behavior in the drift, diffusion volatility and jumps**: All the characteristics in the LAC-JCIR process are scaled by the seasonal activity rate $a(\cdot)$, and hence they all display seasonal behavior. In peak seasons, like summer and winter, while the diffusive volatility and upward jump intensity become higher, the smooth mean-reversion force and downward jump intensity also strengthen to pull back any large deviation from the normal range, thus more spikes are created in these seasons.

- **Consecutive positive spikes**: The LAC-JCIR process is able to generate consecutive positive spikes in peak seasons, a phenomenon that is often observed in many markets in practice. Recall that the jump measure of the LAC-JCIR process has two components (see (7)). The first component gives the intensity for positive jumps from the JCIR process, with its level modulated by $\gamma a(t)$. The second component shows the intensity for mean-reverting jumps created by the time change, and the arrival rate of jumps with size in $[y, y+dy]$ given time t and state x is given by $a(t)\int_{(0,\infty)} p(\tau, x, x+y)\nu(d\tau)dy$, also modulated by $a(t)$. Now imagine that a positive spike has just occurred. In peak seasons, the significant increase in the level of $a(t)$ can create a cluster of positive jumps from the first jump component as well as from the second one (multiple upward jumps in a short time period). Therefore, shortly after the first spike, it is very likely to observe another positive jump which will then be corrected by the mean-reverting jumps and the mean-reverting drift, thus creating the second positive spike. This process can go on, leading to several positive spikes in a row. The likelihood of this pattern clearly increases with the magnitude of $a(t)$. By setting c_1 and c_2 to appropriate levels, our model is very likely to generate consecutive positive spikes. In Section 5, for the New England market where consecutive positive spikes are observed in the summer, our calibration shows that the value of $a(t)$ in the summer is almost three times of its level in the off-peak seasons. The simulated trajectory of the LAC-JCIR model shows consecutive positive spikes in this case (Figure 5 (b)).

We now consider a special specification under our framework with $L_t = t$ (i.e., no Lévy subordination). In this case we call X^ϕ as the AC time-changed JCIR process or AC-JCIR process for short, and its generator $\mathcal{G}_t^\phi$ is given by the following. For $f \in C_c^2(I)$,

$$\mathcal{G}_t^\phi f(x) = \frac{1}{2}a(t)\sigma^2 x f''(x) + a(t)\kappa(1-x)f'(x) + a(t)\frac{\varpi}{\mu}\int_{(0,\infty)}(f(x+y)-f(x))e^{-\frac{y}{\mu}}dy.$$

Similar to the general specification, all the characteristics are seasonal in this process. However, since in this case the time-change T is continuous, the AC-JCIR process *cannot* exhibit mean-reverting jumps, and hence, mean-reversion is solely realized via the smooth mean-reversion force. In Section 5, we will test this specification against the general case to see whether the contribution of jumps to mean-reversion is statistically significant in practice.

Remark 1. *The existence of stochastic volatility in electricity markets is documented in e.g., Escribano et al. (2011). The volatility term in the LAC-JCIR process is local and seasonal, but our modelling framework is flexible enough that it allows us to easily introduce stochastic volatility. Let $(V_t)_{t\geq 0}$, with $V_0 = v \geq 0$, be a non-negative stochastic process independent of L and X (a typical choice for V is the CIR process). We propose two alternatives for the time change T to construct the time-changed process $X_t^\phi = X_{T_t}$:*

(a) Define T as $T_t = L_{A_t} + \int_0^t V_u du$ where $A_t = \int_0^t a(u)du$ as before.

(b) Define T as $T_t = L_{\widetilde{A}_t}$ where $\widetilde{A}_t = \int_0^t (a(u) + V_u)du$.

It can be easily shown that in both specifications, V plays the role of a stochastic volatility factor as in the Heston model. The only difference between these specifications is that (a) introduces the stochastic volatility factor V only into the diffusion component of X^ϕ, while (b) also introduces V into the jump component of X^ϕ, hence the jump intensity is also stochastic (see Mendoza-Arriaga et al. (2010) for details). While adding stochastic volatility improves the realism of the LAC-JCIR process, the new process with stochastic volatility is undoubtedly less parsimonious, more difficult to estimate from data and more computationally demanding for pricing derivatives compared to the LAC-JCIR process. Since the purpose of this paper is to develop a relatively simple and parsimonious electricity price model that captures key features of the prices and is also tractable for pricing various types of derivatives, we do not consider the stochastic volatility specification further in this paper. In Section 5, we will show that the model based on the LAC-JCIR process already provides a good fit to data.

3.2 The Laplace Transform of the GMAC-JCIR Process

We calculate the Laplace transform of the GMAC-JCIR process. The Laplace transform of the JCIR process is well known (see, e.g., Duffie and Gârleanu (2001), Appendix A)

$$\mathbb{E}_x\left[e^{-\lambda X_t}\right] = C(\lambda;t)A(\lambda;t)e^{-B(\lambda;t)x} \tag{11}$$

where

$$A(\lambda;t) = \left[\frac{2\kappa e^{\kappa t}}{2\kappa + (2\kappa + \lambda\sigma^2)(e^{\kappa t} - 1)}\right]^b,\ B(\lambda;t) = \frac{2\kappa\lambda}{2\kappa + (2\kappa + \lambda\sigma^2)(e^{\kappa t} - 1)},$$
$$C(\lambda;t) = \left[e^{-\kappa t} + \frac{(2\kappa + \lambda\sigma^2)(1 - e^{-\kappa t})}{2\kappa(1 + \lambda\mu)}\right]^{-\varpi a},\ a = \frac{2\mu}{\sigma^2 - 2\mu\kappa},\ b = \frac{2\kappa}{\sigma^2}.$$

It follows from (5) that the Laplace transform of X_t^ϕ can be computed as ($\mathbb{E}_{s,x}$ denotes taking expectation under $\mathbb{P}$ conditional on $X_s = x$):

$$\mathbb{E}_{s,x}\left[e^{-\lambda X_t^\phi}\right] = \int_{[0,\infty)} \mathbb{E}_x\left[e^{-\lambda X_u}\right] q_{s,t}(du) \tag{12}$$

Let $g_t(du)$ be the transition probability distribution of a Gamma subordinator with zero drift, mean and variance rate m and v, then $g_t(du)$ is given by the following Gamma distribution:

$$g_t(du) = \frac{(\frac{m}{v})^{\frac{m^2}{v}t}}{\Gamma(\frac{m^2}{v}t)} u^{\frac{m^2}{v}t - 1} e^{-\frac{m}{v}u} du. \tag{13}$$

Now for $T_t = L_{A_t}$ where L is a Gamma subordinator with drift γ, mean and variance rate m and v, (12) becomes

$$\mathbb{E}_{s,x}\left[e^{-\lambda X_t^\phi}\right] = \int_{[0,\infty)} \mathbb{E}_x\left[e^{-\lambda X_{\gamma(A_t - A_s) + u}}\right] g_{A_t - A_s}(du). \tag{14}$$

This integral can be efficiently computed by the Gauss-Laguerre quadrature, i.e.

$$\mathbb{E}_{s,x}\left[e^{-\lambda X_t^\phi}\right] \approx \sum_{i=1}^N w_i \mathbb{E}_x\left[e^{-\lambda X_{\gamma(A_t - A_s) + u_i}}\right] g_{A_t - A_s}(u_i).$$

Typically even with a small number of quadrature points, the quadrature can achieve high level of accuracy. Table 1 provides a numerical example. We set the parameter values according to our calibration results for the jump-diffusion specification for the New England market with $s = 0.2$, $t = s + 1/365$ (i.e. Laplace transform of the state one day ahead) and $x = 0.8$. In this case, using 10 quadrature points we already achieve accuracy to the 10th decimal place.

N	$\lambda = 5$	$\lambda = 10$
5	0.0153786755	0.0003106615
6	0.0153785878	0.0003106632
7	0.0153785743	0.0003106661
8	0.0153785728	0.0003106674
9	0.0153785728	0.0003106679
10	0.0153785729	0.0003106680
11	0.0153785729	0.0003106680
12	0.0153785729	0.0003106680

Table 1: Convergence of the Gauss-Laguerre quadrature for computing the Laplace transform of the LAC-JCIR process

When X^ϕ is the AC-JCIR process, its Laplace transform is particularly simple to calculate, which is given by

$$\mathbb{E}_{s,x}\left[e^{-\lambda X_t^\phi}\right] = \mathbb{E}_x\left[e^{-\lambda X_{A_t - A_s}}\right].$$

This is a major advantage of the AC-JCIR specification.

Remark 2. *Besides the Gamma process, there are other Lévy subordinators that have explicit transition density (e.g. the Inverse-Gaussian process). To compute the Laplace transform of the LAC-JCIR process under these subordinators, one can still apply Gauss quadrature. But now the abscissae and weights must be determined using discretization as the associated orthogonal polynomials are not known (see e.g., Press et al. (1996)). In the Gamma case, the associated orthogonal polynomials for Gauss quadrature are Laguerre polynomials, so the abscissae and weights can be determined easily without discretization. For this reason, we use Gamma subordinator for our model, and we show that it is able to provide good fit to market data in Section 5.*

4 Derivatives Pricing

We price electricity derivatives under an equivalent martingale measure. Since electricity is a non-tradable asset, any probability measure equivalent to the physical measure $\mathbb{P}$ is an equivalent martingale measure (Benth et al. (2008)). In Section 4.1, we introduce a class of equivalent measure changes such that under the new measure $\overline{\mathbb{P}}$, the LAC-JCIR process X^ϕ remains a LAC-JCIR process, but with possibly different parameters (see Proposition 3). Applying these measure changes, the GMAC-JCIR process remains to be a GMAC-JCIR process under the pricing measure and this makes our model tractable for derivative pricing. In general the choice of equivalent martingale measures is not unique. In practice, one can pin down one martingale measure by calibrating the model to observed prices of liquid derivatives. In Section 4.2, for general LAC-JCIR processes, we obtain a closed-form formula for the futures price. We also obtain the Laplace transform of the

futures put option price as a function of the shifted and scaled strike using the Laplace transform of X^ϕ. Hence the put price can be efficiently recovered through Laplace inversion given the Laplace transform of X^ϕ.

4.1 Equivalent Measure Changes

We are in the same setting as Section 3.1. Under $\mathbb{P}$, X^ϕ is a Markov semimartingale on $(\Omega, (\mathcal{F}_t)_{t\geq 0})$, with generating tuple $(\kappa, \sigma, \varpi, \mu, \gamma, \nu(\cdot), a(\cdot))$ and its semimartingale characteristics are given by $(B^\phi, C^\phi, \nu^\phi)$. Consider another tuple $(\overline{\kappa}, \overline{\sigma}, \overline{\varpi}, \overline{\mu}, \overline{\gamma}, \overline{\nu}(\cdot), \overline{a}(\cdot))$, with $\overline{\kappa}, \overline{\sigma}, \overline{\varpi}, \overline{\mu} > 0$, $2\overline{\kappa} \geq \overline{\sigma}^2$, $\overline{\gamma} \geq 0$, $\int_{(0,\infty)} (\tau \wedge 1)\overline{\nu}(d\tau) < \infty$ and $\overline{a}(u)$ is a continuous positive bimodal periodic function with one-year period as in Figure 1 without normalization to be one outside winter and summer. Let $\overline{p}(\tau, x, x+y)$ be the transition probability density of the JCIR process with parameter $(\overline{\kappa}, \overline{\sigma}, \overline{\varpi}, \overline{\mu})$, and $\overline{\phi}(\lambda, u)$ is the density of the Laplace exponent of the additive subordinator, constructed from time changing a Lévy subordinator with parameter $(\overline{\gamma}, \overline{\nu}(\cdot))$ by the activity rate process $\overline{a}(\cdot)$. We can define a triplet of characteristics $(B^{\overline{\phi}}, C^{\overline{\phi}}, \nu^{\overline{\phi}})$ as in (8), (9) and (10) by fixing the truncation function to be $h(x) = x1_{\{|x|\leq 1\}}$. The first question that needs to be addressed is whether there exists a unique probability measure on $(\Omega, (\mathcal{F}_{0,t})_{t\geq 0})$ such that X^ϕ is a semimartingale with characteristics $(B^{\overline{\phi}}, C^{\overline{\phi}}, \nu^{\overline{\phi}})$. The solution to such problem is called the solution to the martingale problem associated with $(B^{\overline{\phi}}, C^{\overline{\phi}}, \nu^{\overline{\phi}})$ (c.f. Jacod and Shiryaev (2003), Definition III.2.4). Obviously, in our case, the solution exists. One can construct a family of probability transition function $p^{\overline{\phi}}(s, t, x, x+y)$ as

$$p^{\overline{\phi}}(s, t, x, x+y) = \int_{[0,\infty)} \overline{p}(\tau, x, x+y)\overline{q}_{s,t}(d\tau)$$

where $\overline{q}_{s,t}(d\tau)$ is the transition probability distribution determined by the Laplace transform $e^{-\int_s^t \overline{\phi}(\lambda,u)du}$. Then a probability measure $\overline{\mathbb{P}}$ can be defined on Ω using $p^{\overline{\phi}}(s, t, x, x+y)$, under which X^ϕ is a semimartingale on $(\Omega, (\mathcal{F}_t)_{t\geq 0})$ with characteristics $(B^{\overline{\phi}}, C^{\overline{\phi}}, \nu^{\overline{\phi}})$ by applying Proposition 2. The remaining question is whether such probability measure is unique. The following lemma provides an affirmative answer.

Lemma 1. *The solution to the martingale problem associated with $(B^{\overline{\phi}}, C^{\overline{\phi}}, \nu^{\overline{\phi}})$ is unique.*

We denote the unique solution by $\overline{\mathbb{P}}$. The next proposition provides sufficient conditions under which $\mathbb{P}$ and $\overline{\mathbb{P}}$ are equivalent.

Proposition 3. *Suppose the following conditions are satisfied,*

(i) $a(s)\gamma \cdot \sigma^2 = \overline{a}(s)\overline{\gamma} \cdot \overline{\sigma}^2$ *for all* $s \geq 0$.

(ii) The Hellinger integral

$$\int_{y\neq 0} \left(\sqrt{\pi^\phi(s, x, y)} - \sqrt{\pi^{\overline{\phi}}(s, x, y)}\right)^2 dy$$

is bounded on $[0, t] \times K$, *for any* $t \geq 0$ *and any compact subset* K *of* I.

Then $\mathbb{P}|_{\mathcal{F}_t} \sim \overline{\mathbb{P}}|_{\mathcal{F}_t}$ *for every* $t \geq 0$.

Note that Condition (i) implies

$$\int_0^t a(s)ds \cdot \gamma \cdot \sigma^2 = \int_0^t \overline{a}(s)ds \cdot \overline{\gamma} \cdot \overline{\sigma}^2, \tag{15}$$

for all $t \geq 0$, i.e., the quadratic variation of the continuous local martingale part does not change. Eq. (15) also implies the equality in (i) must hold for all $s \geq 0$ due to the continuity of $a(s)$ and $\overline{a}(s)$. Next we consider how to verify Condition (ii). Note that when $\int_{(0,\infty)} \nu(d\tau) < \infty$ and $\int_{(0,\infty)} \overline{\nu}(d\tau) < \infty$, i.e., $\nu(\cdot)$ and $\overline{\nu}(\cdot)$ have finite activity, it is automatically satisfied (see Li and Mendoza-Arriaga (2015), Remark 3.1 for details). We next consider the more challenging case where both $\nu(\cdot)$ and $\overline{\nu}(\cdot)$ have infinite activity. In this case both $\pi^{\phi}(s,x,y)$ and $\pi^{\overline{\phi}}(s,x,y)$ go to ∞ as $y \to 0$. From Li and Mendoza-Arriaga (2015) Proposition 4.1, for any $\epsilon > 0$,

$$\int_{|y|>\epsilon} \left(\sqrt{\pi^{\phi}(s,x,y)} - \sqrt{\pi^{\overline{\phi}}(s,x,y)} \right)^2 dy$$

is bounded on $[0,t] \times K$ for any $t > 0$ and any compact set K of I. Thus Condition (ii) depends on the behavior of $\pi^{\phi}(s,x,y)$ and $\pi^{\overline{\phi}}(s,x,y)$ near $y = 0$, and to verify it, we need to study the asymptotic behavior of $\pi^{\phi}(s,x,y)$ as $y \to 0$, which clearly depends on the choice of the subordinator. In the following, we consider the tempered stable family of Lévy subordinators, which includes the Gamma process as a special case. This family is used in Barndorff-Nielsen and Levendorskiĭ (2001) and Boyarchenko and Levendorskiĭ (2002) for modelling equity derivatives. The Lévy measure $\nu(d\tau)$ and the Laplace exponent $\psi(\lambda)$ of this family are given by

$$\nu(d\tau) = C\tau^{-1-p}e^{-\eta\tau}d\tau, \ \psi(\lambda) = \begin{cases} \gamma\lambda - C\Gamma(-p)\left[(\lambda+\eta)^p - \eta^p\right], & 0 < p < 1 \\ \gamma\lambda + C\ln(1+\lambda/\eta), & p = 0 \end{cases}. \tag{16}$$

with $C > 0$, $0 \leq p < 1$, $\eta > 0$. While (16) is the standard parametrization in the literature, a more intuitive way to parameterize the Lévy measure is to use m and v, the mean and variance rate of the stochastic part of the Lévy subordinator (i.e. $m = \mathbb{E}[L_1] - \gamma$ and $v = \mathrm{Var}[L_1]$). For tempered stable Lévy subordinators, C, η and m, v are related as follows.

$$\begin{cases} m = -C\Gamma(-p)p\eta^{p-1}, \ v = -C\Gamma(-p)p(1-p)\eta^{p-2}, & 0 < p < 1 \\ m = \frac{C}{\eta}, \ v = \frac{C}{\eta^2}, & p = 0 \end{cases}.$$

We derive the following explicit conditions which are equivalent to Condition (i) and (ii) for tempered stable subordinators.

Proposition 4. *Suppose $\nu(d\tau)$ is in the tempered stable family. Then Condition (i) and (ii) in Proposition 3 are equivalent to the following:*

$$p = \overline{p}, \ a(s)\gamma \cdot \sigma^2 = \overline{a}(s)\overline{\gamma} \cdot \overline{\sigma}^2, \ a(s)C\sigma^{2p} = \overline{a}(s)\overline{C}\overline{\sigma}^{2p} \text{ for all } s \geq 0. \tag{17}$$

Proposition 4 implies that, for tempered stable Lévy subordinators, under the class of equivalent measure changes we consider, $\overline{a}(s)$ should be a constant multiple of $a(s)$. If we require the value of $\overline{a}(s)$ to be one in periods outside summer and winter, then $a(s) = \overline{a}(s)$ for all s. For the remaining parameters, κ, ϖ, μ, η can be changed freely, while γ, σ, C and p must satisfy (17).

4.2 Pricing Electricity Futures Contracts and European-style Futures Options

We now work under the equivalent martingale measure $\overline{\mathbb{P}}$ obtained by calibrating the model to the market. Under $\overline{\mathbb{P}}$, the parameters of X^ϕ are denoted with an overhead bar and taking expectation under $\overline{\mathbb{P}}$ is denoted by $\overline{\mathbb{E}}$. In electricity markets, unlike other markets, delivery for a futures contract is made over a specified time period. Let $F(t, T_1, T_2)$ $(t < T_1 < T_2)$ be the futures price at time t for delivery between T_1 and T_2. The futures price is given by (see Lucia and Schwartz (2002) or Benth et al. (2008)):

$$F(t, T_1, T_2) = \frac{1}{M}\overline{\mathbb{E}}\left[\sum_{i=0}^{M} S_{T_1+ih}\middle|\mathcal{F}_t\right],$$

where $h = 1/365$ year and $T_2 - T_1 = Mh$ for some positive integer M, i.e. there are M days in $(T_1, T_2]$.

Proposition 5. *Under our model, the futures price $F(t, T_1, T_2)$ is given by*

$$F(t, T_1, T_2) = A(t, T_1, T_2)X_t^\phi + B(t, T_1, T_2) \tag{18}$$

where

$$A(t, T_1, T_2) = \frac{1}{M}\sum_{i=0}^{M} \Lambda(T_1 + ih)e^{-\overline{\psi}(\overline{\kappa})\int_t^{T_1+ih}\overline{a}(u)du},$$

$$B(t, T_1, T_2) = \frac{1}{M}\left(1 + \frac{\overline{\mu}\cdot\overline{\varpi}}{\overline{\kappa}}\right)\sum_{i=0}^{M} \Lambda(T_1 + ih)\left(1 - e^{-\overline{\psi}(\overline{\kappa})\int_t^{T_1+ih}\overline{a}(u)du}\right).$$

Note that the futures formula holds for any Lévy subordinator. Here $\overline{\psi}$ is the Laplace exponent of the Lévy subordinator under the pricing measure and it is given by a simple closed-form formula for many subordinators, including in particular the Gamma process (see Eq.(3)). The integral $\int_t^{T_1+ih}\overline{a}(u)du$ can also be calculated in closed-form for our specification of the activity rate (see Figure 1). Hence the futures formula under our model is particularly simple to evaluate.

We next consider how to price a European-style option on the electricity futures contract. We assume the risk-free rate is a positive constant, denoted by r. We only consider how to price a put option, and the call option price can be easily obtained from the put-call parity. Let K be the strike price and T be the maturity time of the option $(T \le T_1)$, written on a futures contract with delivery period $[T_1, T_2]$. At time t $(t \le T)$ the put option price $P(K, t, T, T_1, T_2)$ is given the following:

$$P(K, t, T, T_1, T_2) = e^{-r(T-t)}\overline{\mathbb{E}}\left[(K - F(T, T_1, T_2))^+\middle|\mathcal{F}_t\right].$$

Let $k = (K - B(T, T_1, T_2))/A(T, T_1, T_2)$. From (18), the put price can be rewritten as:

$$P(k, t, T, T_1, T_2) = e^{-r(T-t)}A(T, T_1, T_2)\overline{\mathbb{E}}\left[(k - X_T^\phi)^+\middle|\mathcal{F}_t\right]. \tag{19}$$

The next proposition shows that when $k \le 0$, the put price is zero and when $k > 0$, it obtains a closed-form expression for the Laplace transform of the put price using k as the transform variable. The put option can then be efficiently and accurately recovered using a fast and accurate Laplace inversion algorithm, such as the one by Abate and Whitt (1992).

Proposition 6. *If* $K \leq B(T, T_1, T_2)$, $P(K, t, T, T_1, T_2) = 0$. *If* $K > B(T, T_1, T_2)$, *define*

$$L_P(\lambda) := \int_0^\infty e^{-\lambda k} P(k, t, T, T_1, T_2) dk, \ \lambda > 0,$$

which is the Laplace transform of the put price as a function of k. *Then given* $X_t^\phi = x$,

$$L_P(\lambda) = e^{-r(T-t)} A(T, T_1, T_2) \frac{1}{\lambda^2} \overline{\mathbb{E}}_{t,x} \left[e^{-\lambda X_T^\phi} \right]. \tag{20}$$

Below we provide numerical examples under two sets of parameters for the GMAC-JCIR model. For the first set of parameters, we use calibration results for the New England market but set $\kappa = 5$. In the second set, we set $\kappa = 10$, $m = 1.2$, $v = 0.8$ and values for the other parameters are the same as the calibration results for the New-England market. We consider an at-the-money put option with $t = 0.3$, $T = 0.8 - 1/52$, $T_1 = 0.8$, $T_2 = 0.8 + 1/12$, i.e. the underlying futures contract matures in 6 months with one-month delivery period and the option matures one week before the futures contract. We set $X_t^\phi = 1.2$ and the corresponding futures price $F(t, T_1, T_2) = 75.81$ and 59.42 for the first and second set of parameters respectively. The put price is calculated by numerically inverting the Laplace transform in (20) using the Abate-Whitt algorithm with 35 terms, and the Laplace transform of the GMAC-JCIR process is computed by the Gauss-Laguerre quadrature with N quadrature points. The benchmark is obtained using 150 terms in the Abate-Whitt algorithm and 100 quadrature points. Results are displayed in Table 2. Typically for option prices, a relative error on the order of 0.1% is good enough in applications. Clearly even with just 5 quadrature points, we have already achieved a high level of accuracy.

N	Put Price	Abs Error
5	4.8228301760	4.2579E-11
6	4.8228301761	1.0099E-12
7	4.8228301761	2.9310E-14
Benchmark	4.8228301761	

N	Put Price	Abs Error
5	3.5867756641	3.7741E-05
6	3.5867873432	2.6062E-05
7	3.5867958564	1.7548E-05
Benchmark	3.5868134048	

Table 2: Absolute error for the put price for different number of quadrature points under two sets of parameters.

Our model is further computationally tractable for options with early exercise and barrier features. Given the Laplace transform of the GMAC-JCIR process, the characteristic function $E_{s,x}[e^{iuX_t^\phi}]$ can be obtained by replacing $-\lambda$ with iu. With the knowledge of the characteristic function, one can apply the efficient Fourier-cosine algorithm developed by Fang and Oosterlee (2009) for Bermudan and barrier options, and by Zhang and Oosterlee (2013) for swing options.

5 Model Calibration and Examples

In this section, we first discuss how to calibrate our model from electricity spot prices and then we show its performance by calibrating to the data from two major electricity markets in the US.

5.1 Calibration Procedure

The calibration procedure consists of two steps. The first step estimates the trend function $\Lambda(t)$ defined in (1), which can be done via the standard technique in the literature (see, e.g., Geman and Roncoroni (2006) and Meyer-Brandis and Tankov (2008)). To adjust for the influence of large spikes, we bound the data series by a suitable quantile of their empirical distribution, and the trend function is fitted to the adjusted data using the least squares method. After obtaining an estimate for $\Lambda(t)$, which is denoted by $\widehat{\Lambda}(t)$, we can turn the spot price data series into a time series for the GMAC-JCIR process X^ϕ by setting $X^\phi_t = S_t/\widehat{\Lambda}(t)$.

In the second step, we estimate the parameters of X^ϕ. We observe that in general, the GMAC-JCIR process X^ϕ has the following scale-invariance property. Recall that γ, m and v are the drift, mean rate and variance rate of the Gamma process, respectively.

Proposition 7. *For any $c > 0$, $(\kappa, \sigma, \varpi, \mu, \gamma, m, v, a(\cdot))$ and $(c\kappa, \sqrt{c}\sigma, c\varpi, \mu, \frac{1}{c}\gamma, \frac{1}{c}m, \frac{1}{c^2}v, a(\cdot))$ give the same probability law for X^ϕ.*

Proposition 7 implies that from the observations of X^ϕ, we can only identify the parameters up to a constant. Hence, in our calibration we set $\gamma = 1$ for the jump-diffusion specification (i.e., $\gamma > 0$) and $m = 1$ for the pure-jump specification (i.e., $\gamma = 0$) to fix the scale. In the activity rate function $a(\cdot)$, we assume time $t = 0$ is the beginning of a winter period, and we set $t_{p1} = \frac{1.5}{12}$, $t_{p2} = \frac{7.5}{12}$, and $\tau_1 = \tau_2 = \frac{1.5}{12}$, since in the examples we consider, spikes are concentrated in summer and winter, and typically they are clustered around the middle of summer and winter. We next estimate the remaining parameters, which are $(\kappa, \sigma, \varpi, \mu, m, v, c_1, c_2)$ in the jump-diffusion case and $(\kappa, \sigma, \varpi, \mu, v, c_1, c_2)$ in the pure-jump case. Availability of the Laplace transform of X^ϕ allows us to estimate the parameters via two methods. In the first approach, we can recover the transition probability density of X^ϕ through an efficient numerical Laplace inversion algorithm such as the one by Abate and Whitt (1992), and then estimate the parameters through maximum likelihood estimation (MLE). Alternatively, we can use the empirical characteristic function (ECF) method of Singleton (2001), which derives estimators directly using the characteristics function, and it achieves the efficiency of MLE asymptotically (note that for our model knowing the Laplace transform is equivalent to knowing the characteristic function). Computationally, the ECF method can be more efficient than MLE, especially in high dimensions since it does not require inversion to obtain the density. Nevertheless, we adopt the MLE approach in our calibration for two reasons. First, our model is one-dimensional and Laplace inversion can be done fast and accurately in our case. Second, the MLE approach allows us to test various interesting hypotheses using the likelihood ratio test and compare different specifications by information criteria like AIC and BIC.

5.2 Calibration Examples

We calibrate our model to two major power markets in the US, namely, the New England (NE) market and the Midwest (MW) market. For each market, we download daily data for the day-ahead average prices from Bloomberg for the 3-year period from Nov 30, 2009 to Nov 30,

2012, including the weekends. The spot prices for these two markets are plotted in Figure 5 (a) and Figure 6 (a). Clearly, they are very different in the spike magnitude with spikes in the New England market being much larger. Therefore, one could think of these markets as representative examples of "high-pressure" and "low-pressure" markets.

We first estimate the trend function. To adjust for the influence of large spikes, we bound the data by the 70% quantile of the empirical distribution as in Geman and Roncoroni (2006). Choices of other quantiles do not significantly affect the results for the trend function. Since it is possible that seasonality occurs annually, semi-annually, quarterly, monthly and weekly, we set $n = 5$ and $f_1 = 1$, $f_2 = 2$, $f_3 = 4$, $f_4 = 12$ and $f_5 = 52$, respectively. The parameters are estimated by ordinary least-squares (OLS). We carried out Durbin-Watson test and Breusch-Pagan test to detect autocorrelation and heteroskedasticity in the residuals, and the test results confirm significance of these phenomena (the p-value is less than 1.0E-8 in both tests for both markets). From the Q-Q plot of the residuals, we also see that the residuals do not follow the normal distribution. We calculate the standard error of the estimates using estimators that are robust to autocorrelated and heteroscedastic residuals. Table 3 displays the estimated parameter values, the t-statistics and the p-value. The estimated trend is plotted in green in Figure 5 and Figure 6. The results indicate that for both markets, monthly seasonality is not significant and for the New England market, quarterly seasonality is also not present. From the magnitude of a_i, for New England annual seasonality prevails while for Midwest semi-annual seasonality is the strongest. The sign of b_0 shows that in the three-year sampling period, in addition to seasonality, the price trend experiences a slight decrease.

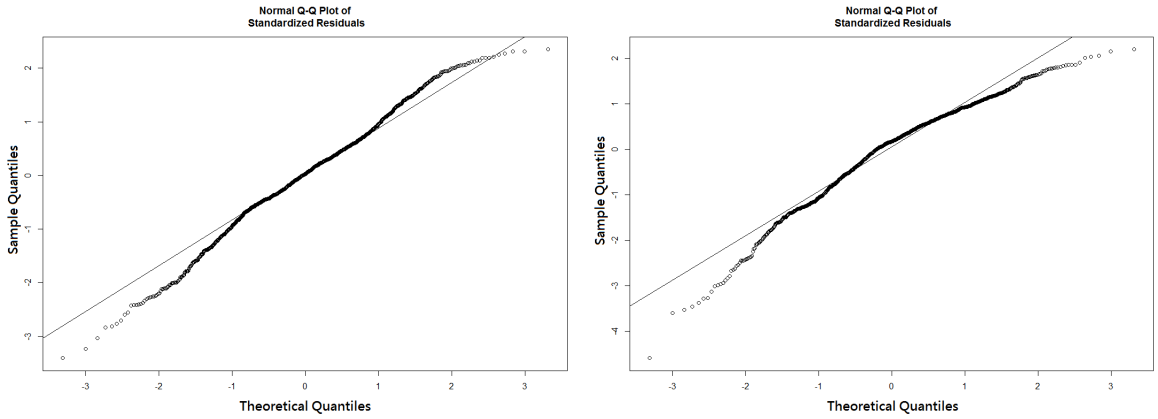

(a) New England (b) Midwest

Figure 3: Q-Q plot of Residuals of New England and Midwest

Given the trend function we obtain the time series for the deseasonalized process X^ϕ. In Figure 4 we plot the annualized rolling historical volatility for the log return of X^ϕ with a rolling window of 30 days for the New England market. A clear seasonal pattern is observed, which suggests the necessity of modelling seasonality in the volatility. This is an issue that has not been addressed in one-dimensional Markov models for electricity prices in e.g., Geman and Roncoroni (2006) and Kjaer (2008), which assume the volatility is constant.

We estimate the parameters of the GMAC-JCIR process X^ϕ by the maximum likelihood method. Results are displayed in Table 4 (standard errors of the estimates are presented in parentheses). For

	New England			Midwest		
	estimates	t-statistics	p-value	estimates	t-statistics	p-value
a_0	3.8583	129.49	0.00E+00	3.5705	243.45	0.00E+00
b_0	-0.1310	-5.83	7.22E-09	-0.0606	-6.11	1.35E-09
a_1	0.0918	2.88	4.08E-03	-0.0372	-2.87	4.18E-03
b_1	0.9625	4.09	4.59E-05	-0.9917	-3.15	1.68E-03
a_2	0.0744	3.09	2.05E-03	0.0527	4.15	3.55E-05
b_2	-1.4080	3.95	8.22E-05	-1.0648	-4.86	1.31E-06
a_3	-0.0362	-1.51	0.133	-0.0323	-2.85	4.41E-03
b_3	-1.0680	-1.64	0.102	-1.0943	-2.94	3.31E-03
a_4	0.0017	0.17	0.861	-0.0045	-0.48	0.631
b_4	0.4047	0.08	0.938	1.9037	0.86	0.391
a_5	0.0226	4.01	6.48E-05	0.0339	6.18	8.82E-10
b_5	0.4301	1.84	0.066	0.0597	0.27	0.791

Table 3: Estimation results for the trend function $\Lambda(t)$.

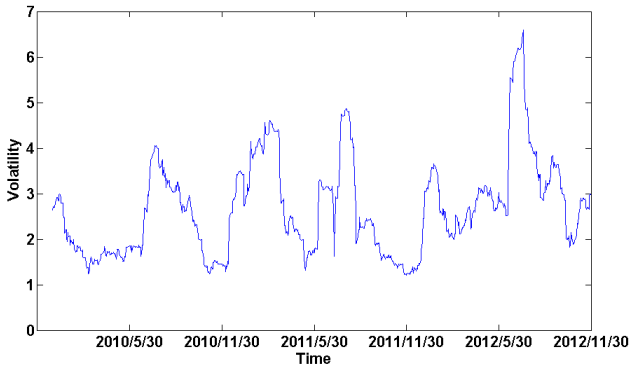

Figure 4: The annualized rolling historical volatility of the log return of deseasonalized prices in New England

the New England market, the jump-diffusion (JD) specification achieves the maximum likelihood while for the Midwest market, the pure-jump (PJ) specification attains the maximum likelihood. Recall that due to scaling invariance, in the JD case we set $\gamma = 1$ and in the PJ case we set $m = 1$.

	GMAC-JCIR		AC-JCIR	
	New England	Midwest	New England	Midwest
κ	25.4924 (8.0568)	128.3875 (17.1987)	77.6725 (7.5533)	113.3108 (11.9951)
σ	1.2665 (0.2055)	2.5709 (0.1312)	2.1665 (0.0724)	2.4243 (0.0830)
ϖ	10.8253 (4.3166)	50.8181 (20.1961)	27.0497 (6.3062)	50.2732 (15.9269)
μ	0.3516 (0.0600)	0.1799 (0.0440)	0.3914 (0.0662)	0.1749(0.0351)
γ	1.0000	0.0000	N.A.	N.A.
m	2.2790 (1.0627)	1.0000	N.A.	N.A.
v	0.0297 (0.0180)	0.0012 (0.0003)	N.A.	N.A.
c_1	0.7823 (0.3041)	1.00E-06(0.2620)	1.3156 (0.3218)	4.00E-06(0.0003)
c_2	1.9239 (0.5291)	0.5614 (0.3079)	3.5419 (0.6599)	0.8161 (0.2912)

Table 4: Estimation results for the GMAC-JCIR and the AC-JCIR process (standard errors are shown in parentheses)

We plot in Figure 5 (a) and 6 (a) the observed price path for the New England market and the Midwest market. It is clear that prices in New England are much more volatile and have much larger spikes than in Midwest. Economically, this is due to the differences in the market fundamentals. Midwest has much larger generating capacity and capacity reserve than New England. Furthermore, coal is the primary fuel for generation in Midwest while in New England, natural gas is used, which is more expensive. Consequently, when demand or supply shocks occur, their influence can die away quickly in Midwest without causing huge price hikes due to sufficient capacity reserve and low-cost fuel. These observations are reflected in our estimated parameter values. Comparing the value of κ and μ in the AC-JCIR specification, which are the mean-reversion speed and the average jump size in the background JCIR process, one can see that in Midwest mean-reversion is much stronger and the mean upward jump size is much smaller (we do not compare mean-reversion and average upward jump size under the GMAC-JCIR specification as one cannot directly compare them for a jump-diffusion and a pure-jump process). From the observed price path for both markets, one can see that spikes are concentrated in both summer and winter for New England, but mainly in summer for Midwest. Our estimation results are consistent with this observation. For New England, both c_1 and c_2 are significantly different from zero while for Midwest, $c_1 \approx 0$ and c_2 is positive. Lastly, we observe that the values of κ, σ, ϖ, c_1 and c_2 for New England are significantly larger under the AC-JCIR specification than under the GMAC-JCIR specification. The reason for this difference is that the AC-JCIR specification only permits upward jumps. This means that, after an upward jump occurs, the process X^ϕ must quickly return to the normal range via diffusion in order to be able to generate spikes. Consequently, κ must be significantly larger under the AC-JCIR specification. Similarly, σ, ϖ, c_1 and c_2 are found to be significantly larger under the AC-JCIR specification as they need to compensate for the lack of large spike-like movements generated by the infinite activity mean-reverting jump measure $\pi^\phi(t, x, y)dy$ available under the GMAC-JCIR specification.

To check whether our model is able to capture the trajectorial features of electricity prices, we plot in Figure 5 (b) and 6 (b) a simulated sample path under the estimated parameters in Table 4. The simulation is done using the exact simulation scheme in Appendix A. These graphs show that our model can reproduce mean-reversion and seasonal spikes very well.

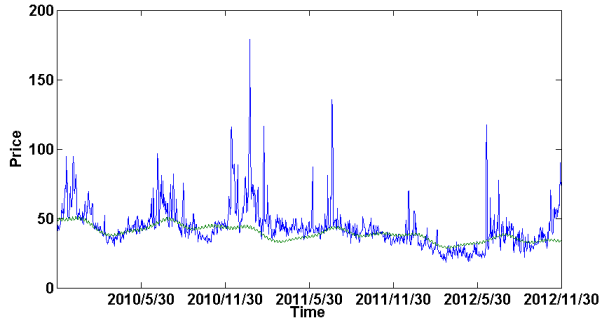

(a) Market price path

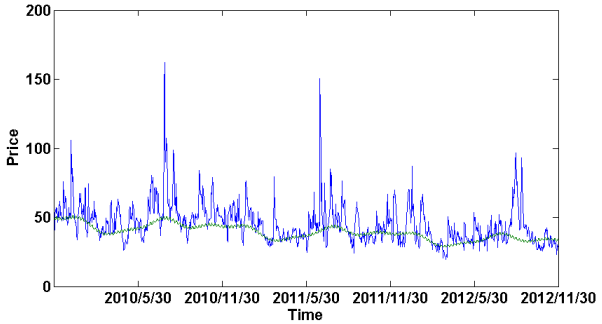

(b) Simulated price path

Figure 5: The New England market price path and simulated price path under the GMAC-JCIR process

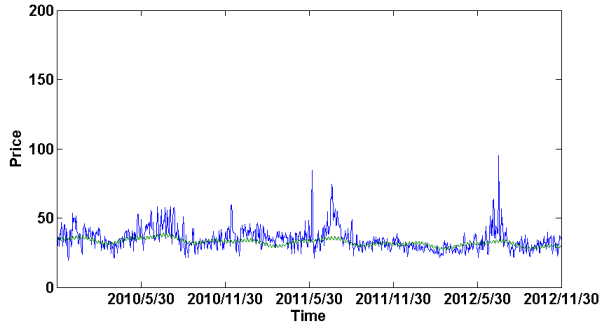

(a) Market price path

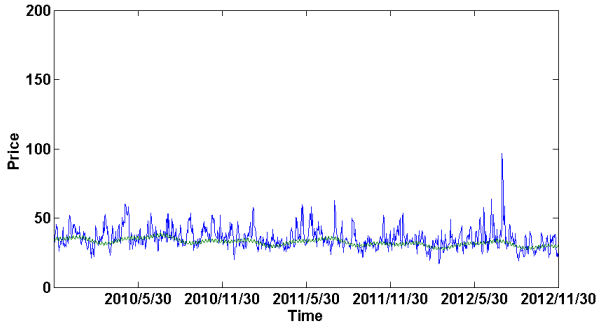

(b) Simulated price path

Figure 6: The Midwest market price path and simulated price path under the GMAC-JCIR process

In the following, we consider several alternative specifications which are special cases under our modelling framework to answer the following three questions for the markets under consideration.

- Q1: Do spikes concentrate in summer and/or winter? By setting $c_1 = c_2 = 0$, the activity rate does not show any seasonality. This special case corresponds to spikes without seasonal features.

- Q2: Do mean-reverting jumps exist? Under the AC-JCIR specification there exist only upward jumps, and hence, the mean-reversion is solely carried out by the continuous drift term. While this specification is also able to reproduce spikes (see Figure 7 for the simulated price paths under parameters obtained from calibrating the AC-JCIR model to data; the calibrated parameter values are shown in Table 4), we want to see statistically how it compares to the GMAC-JCIR model where mean-reverting jumps are present.

- Q3: For the GMAC-JCIR process, should we use the JD specification or the PJ one? Given that jumps in the GMAC-JCIR have infinite activity and the PJ specification can produce both small frequent moves and large rare moves, the necessity of having a diffusion component becomes questionable. The same question has been examined under the CGMY model for various stock indexes and stocks in Carr et al. (2002).

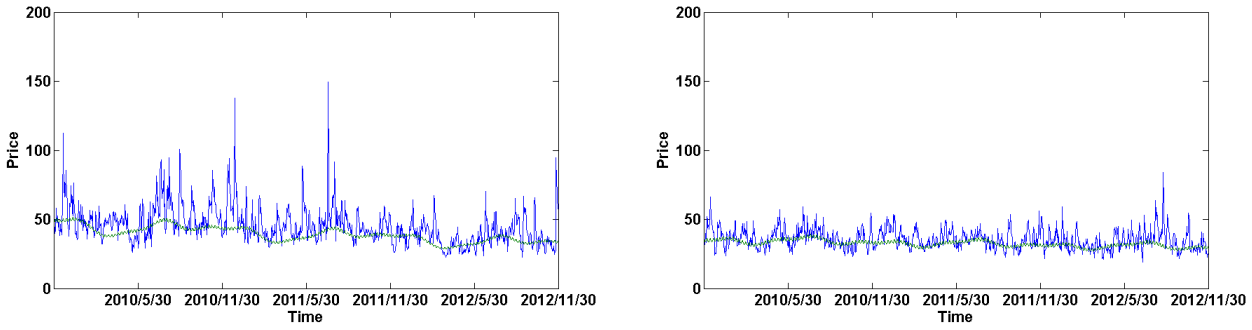

(a) Simulated price path for New England

(b) Simulated price path for Midwest

Figure 7: Simulated price paths under the AC-JCIR process

We address these questions in two ways. First, we formulate them as null hypotheses and test them by the likelihood ratio test as the maximum likelihood value for each null hypothesis and the full model is available (the likelihood ratio follows the Chi-square distribution asymptotically; see Billingsley (1961) for the statistical inference theory for Markov processes). The null hypothesis H_0 for each question is listed as follows.

- For Q1, $H_0 : c_1 = c_2 = 0$.
- For Q2, $H_0 : m = 0$ (A Lévy subordinator with zero mean for all t is deterministic, and hence $m = 0$ implies $v = 0$).
- For Q3, $H_0 : \gamma = 0$.

Second, we compare different specifications by AIC and BIC. These information criteria consider model parsimony and penalize increase in the likelihood value by extra number of parameters. The degree of penalty imposed by AIC and BIC is different with the penalty in BIC being stronger.

Values for the likelihood ratio as well as for AIC and BIC are displayed in Table 5 for the New England market and in Table 6 for the Midwest market. "Reject" means rejecting H_0. The likelihood ratio test is carried out at 5% significance level, and the 95% quantile of the Chi-Square distribution with one and two degrees of freedom are 3.84 and 5.99 respectively. For AIC and BIC, the model with smaller value is preferred. For each null hypothesis, the first row displays AIC and BIC values under H_0 while the second row shows values under the full model. We do not do tests for the third question in the Midwest market as the PJ specification achieves the maximum likelihood value.

For the New England market, the likelihood ratio test results indicate the seasonal occurrence of spikes as well as the presence of mean-reverting jumps and a diffusion component are statistically significant. With the penalty for extra parameters, the jump-diffusion GMAC-JCIR model is better

	Likelihood Ratio	AIC	BIC
$H_0 : c_1 = c_2 = 0$	36.46	-1155.84	-1125.84
		-1188.30	-1148.30
	Reject	Reject	Reject
$H_0 : m = 0$	74.62	-1117.69	-1087.68
		-1188.30	-1148.30
	Reject	Reject	Reject
$H_0 : \gamma = 0$	4.69	-1185.61	-1150.61
		-1188.30	-1148.30
	Reject	Reject	Accept

Table 5: Likelihood ratio, AIC and BIC for New England

	Likelihood Ratio	AIC	BIC
$H_0 : c_1 = c_2 = 0$	5.69	-1356.86	-1331.86
		-1358.55	-1323.55
	Accept	Reject	Accept
$H_0 : m = 0$	18.60	-1341.95	-1311.95
		-1356.55	-1316.54
	Reject	Reject	Reject

Table 6: Likelihood ratio, AIC and BIC for Midwest

than more parsimonious specifications except that the pure-jump specification is preferred when looking at BIC, which imposes stronger penalty on extra number of parameters.

For the Midwest market, the seasonal occurrence of spikes is not significant at the 5% level, but the value of the likelihood ratio, 5.69, is close to the threshold 5.99. In fact, H_0 is rejected if the significance level is increased to 6%. For this market, we can conclude that there is some statistical evidence of seasonality in spikes. The presence of mean-reverting jumps is statistically significant and the GMAC-JCIR model is preferred over the AC-JCIR model even when the extra parameters are penalized.

Next we assess how our model captures the statistical properties of market data. To do this, we follow the usual practice in the literature (see e.g. Geman and Roncoroni (2006) and Benth et al. (2012)) to compare the simulated moments of daily log returns with the empirical moments, and the results are displayed in Table 7. To calculate the simulated moments, we simulate 10000 sample paths in the three-year sampling period under the calibrated parameter values of each model, and for each path, we obtain a sample of daily price log returns and calculate its mean, standard deviation, skewness and kurtosis. Then for each moment, the values of that moment in all sample paths are averaged to produce the simulated value.

New England	Empirical	GMAC-JCIR	AC-JCIR	MRJD
Average	5.99E-04	-2.79E-05	-3.54E-05	-1.23E-04
Stdev	0.1502	0.1610	0.1716	0.1608
Skewness	0.2000	1.1598	1.2372	-0.0610
Kurtosis	7.7458	8.6988	8.0706	9.6344
Midwest	**Empirical**	**GMAC-JCIR**	**AC-JCIR**	**MRJD**
Average	1.72E-04	1.05E-04	1.15E-04	6.79E-05
Stdev	0.1402	0.1414	0.1409	0.1336
Skewness	0.4177	0.4364	0.4916	0.3165
Kurtosis	4.1553	4.9532	4.3858	5.9041

Table 7: Moment Matching

We compare our model to the popular model of Cartea and Figueroa (2005), where the deseasonalized price X is assumed to follow

$$d\ln X_t = -\kappa \ln X_t dt + \sigma dB_t + J dq_t,$$

where $\kappa, \sigma > 0$, $J \sim N(\mu_J, \sigma_J^2)$ and q is a Poisson process with arrival rate λ. We follow the literature to call it as the mean-reverting jump-diffusion (MRJD) model. In the original formulation in Cartea and Figueroa (2005), they assume the diffusion volatility is a time-dependent function, denoted by $\sigma(t)$. However, they do not specify any functional form for it, and simply use the rolling historical volatility as a substitute. That is, at any time t in the sampling period, they estimate $\sigma(t)$ by the rolling historical volatility at time t. Thus we only know $\sigma(t)$ in the sampling period. However, in the following we want to do out-of-sample prediction and need to calculate the conditional expectation $E[S_{t+h}|\mathcal{F}_t]$, which requires the value of the volatility function $\sigma(u)$ in

the out-of-sample period $(t, t+h]$. In order to use the MRJD model for prediction, we assume $\sigma(t)$ is constant. We estimate the model parameters using the method in Cartea and Figueroa (2005), with σ estimated by the average of the rolling historical volatility (see Benth et al. (2012)). The estimated parameter values are shown in Table 8. Standard errors, when available, are given in parentheses.

	New England	Midwest
κ	74.0879 (7.8865)	125.2408 (10.9371)
σ	2.6821	2.5527
λ	12	4.3333
μ_J	-0.0129 (0.0857)	0.1816 (0.1230)
σ_J^2	0.2642 (0.0632)	0.1967 (0.0803)

Table 8: Estimation results for the MRJD model

The simulated moments of the MRJD are displayed in Table 7. For the first two moments, all models match the empirical moments quite well. For skewness and kurtosis, the MRJD model tends to underestimate skewness while overestimate kurtosis quite significantly for both markets. In contrast, the GMAC-JCIR and AC-JCIR model provide a more satisfactory matching of these moments. The only exception is the matching of the skewness in the New England market, for which the GMAC-JCIR and AC-JCIR overestimates the skewness. This suggests that mean-reversion ought to be more pronounced in these models for this market. For the Midwest market, the GMAC-JCIR model provides a very close match of the skewness.

Remark 3. *We have also calculated the simulated autocorrelation function under the GMAC-JCIR, AC-JCIR and MRJD models. Comparing to the empirical autocorrelation function from the market, all three models are able to match the empirical autocorrelation for short time lags quite closely. However, for large time lags, the empirical autocorrelation remains to be strong and the autocorrelation from all the models does not provide a good match. The result is not surprising as all the models considered here only employ a single Markovian factor. To improve the fit for auto-correlation, one can extend the current single factor Markovian framework by adding more factors, i.e., one can assume the deseasonalized spot price is a product of several positive and independent factors. Meyer-Brandis and Tankov (2008) considered a two-factor model using Non-Gaussian OU processes to model the factors and show that it is able to fit the empirical autocorrelation function well. Here, one can use the GMAC-JCIR or AC-JCIR process to model the factors. While the multi-factor model can improve the fit, to estimate it and to price electricity derivatives require a lot more computational efforts compared to the single factor case. Since the primary goal of this paper is to develop a relatively simple and parsimonious electricity price model that captures key features of the prices and is also tractable for pricing various types of electricity derivatives, we do not pursue such extension here and will leave it for future research.*

We also compare these models by looking at out-of-sample prediction errors for the spot price in the period from Dec 1, 2012 to Nov 30, 2013. At any time t in this period, we predict the price at time $t+h$ using the conditional expectation $E[S_{t+h}|\mathcal{F}_t]$, which is the best prediction in the mean-square sense. Its value is calculated using the parameter values calibrated from the 3-year sampling period. For the prediction interval h, we use 1 day, 7 days and 30 days, representing short, medium and long term. Let $e_i = |E[S_{t_i+h}|\mathcal{F}_{t_i}] - S_{t_i+h}|$. We measure the overall prediction

error by the Root Mean Squared Error (RMSE) and Mean Absolute Percentage Error (MAPE) defined as follows:

$$\text{RMSE} = \sqrt{\frac{1}{N}\sum_{i=1}^{N} e_i^2}, \quad \text{MAPE} = \frac{1}{N}\sum_{i=1}^{N} \frac{e_i}{S_{t_i+h}}.$$

For $h = 1, 7, 30$ days, we have $N = 365, 358, 335$, respectively. The results show that all three models are quite close for 1-day prediction, with the GMAC-JCIR model being the best in terms of RMSE and the MRJD model being slightly better than the other two models in terms of MAPE. However as the prediction horizon increases, both the GMAC-JCIR and the AC-JCIR model perform better than the MRJD model under both RMSE and MAPE. The difference is particularly obvious for the New England market which has large spikes. The prediction errors for New England are much larger than those for Midwest. This is because big spikes with magnitude even greater than those observed in the sampling period occur in the prediction period (see Figure 8).

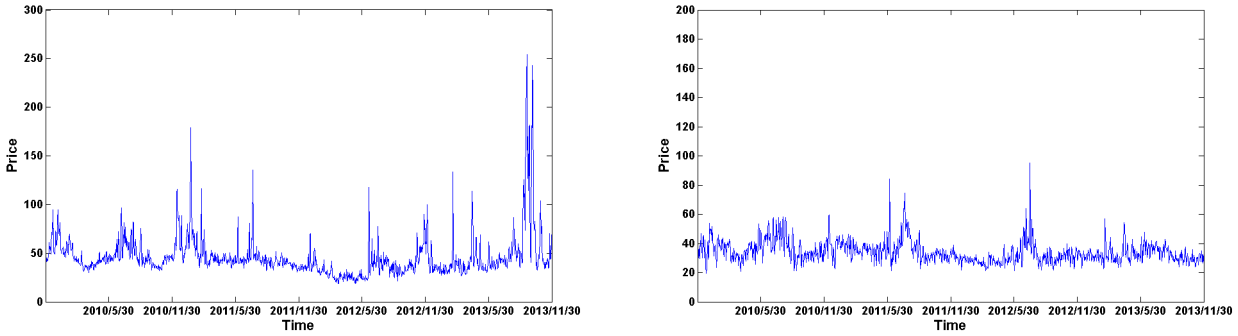

(a) New England (b) Midwest

Figure 8: Market price path in the sampling and prediction period

New England	RMSE				MAPE		
	GMAC-JCIR	AC-JCIR	MRJD		GMAC-JCIR	AC-JCIR	MRJD
1-day	18.0825	19.1414	18.9170	1-day	14.24%	14.45%	14.16%
7-days	36.9585	37.9958	38.2313	7-days	22.26%	22.70%	24.73%
30-days	41.1684	41.3546	42.8999	30-days	26.30%	26.59%	30.14%
Midwest	RMSE				MAPE		
	GMAC-JCIR	AC-JCIR	MRJD		GMAC-JCIR	AC-JCIR	MRJD
1-day	3.8975	3.9028	3.9436	1-day	8.92%	8.95%	8.87%
7-days	5.5565	5.4911	6.0567	7-days	12.37%	12.32%	12.88%
30-days	5.9336	5.8786	6.5283	30-days	13.15%	13.13%	13.89%

Table 9: Prediction Errors

To check the statistical significance of the difference in the prediction error among these three

models, we perform the Diebold-Mariano (DM) test (see Diebold and Mariano (1995)). Table 10 shows the p-value for the test. We consider two loss functions. One is the squared error, and the other is the absolute percentage error (APE). The null hypothesis is that model 1 and 2 have the same prediction accuracy while the alternative hypothesis is that model 1 is more accurate than model 2. In Table 10, the name of model 1 appears first while the name of model 2 is given after the hyphen.

New England	Squared Error		
	GMAC-JCIR vs AC-JCIR	GMAC-JCIR vs MRJD	AC-JCIR vs MRJD
1-day	2.86E-04	0.029	0.743
7-days	7.32E-07	5.32E-12	0.043
30-days	2.01E-18	1.95E-20	1.07E-20

Midwest	Squared Error		
	GMAC-JCIR vs AC-JCIR	GMAC-JCIR vs MRJD	AC-JCIR vs MRJD
1-day	0.276	0.136	0.206
7-days	1.000	5.68E-14	1.93E-13
30-days	1.000	4.19E-16	3.60E-15

New England	APE		
	GMAC-JCIR vs AC-JCIR	GMAC-JCIR vs MRJD	AC-JCIR vs MRJD
1-day	0.053	0.676	0.887
7-days	1.17E-04	5.63E-12	3.94E-10
30-days	6.59E-09	7.76E-22	2.32E-23

Midwest	APE		
	GMAC-JCIR vs AC-JCIR	GMAC-JCIR vs MRJD	AC-JCIR vs MRJD
1-day	0.063	0.746	0.795
7-days	0.948	8.53E-03	0.010
30-days	0.729	8.70E-04	2.10E-03

Table 10: p-Values for the DM Test

We consider the significance level to be 5%. The test results indicate that for 1-day prediction, the difference in the prediction error is statistically insignificant except that when using the squared error as the loss function, the GMAC-JCIR model is better than the other two. However as the prediction horizon increases, both the GMAC-JCIR and the AC-JCIR model are significantly better than the MRJD model using both loss functions. Comparing the GMAC-JCIR and the AC-JCIR model, that the former is better than the latter is statistically significant for the New England market but one cannot reject the null hypothesis that they have the same accuracy for the Midwest market.

Finally, the GMAC-JCIR and the AC-JCIR model are more tractable than the MRJD model

for derivatives valuation. The futures formula under our model is particularly simple to evaluate while the analytical formula for the futures price obtained in Cartea and Figueroa (2005) requires numerical evaluation of integrals. Furthermore, using Gauss-Laguerre quadrature and Abate-Whitt inversion, futures options can be priced efficiently with high level of accuracy under our model. To our best knowledge, under the MRJD model, pricing futures option needs to be done by numerical PIDE methods, which typically require a large number of time steps and space nodes to achieve a high level of accuracy.

6 Conclusions

This paper proposes a new stochastic model for electricity spot prices based on time changing the JCIR process, where the random clock is a Gamma subordinator time changed by a deterministic clock with seasonal activity rate. Our model differs from existing one-dimensional Markov models for electricity prices in several ways. *First*, compared to classical jump-diffusion models where mean reversion can only be realized via the smooth mean-reversion force in the drift term, we also allow jumps to contribute to mean reversion. *Second*, compared to the threshold model of Geman and Roncoroni (2006), upward jumps are possible even when the spot price is already very high, a phenomenon that can be observed in practice. *Third*, under our model the drift, diffusion volatility and jumps are all seasonal which are empirically supported in markets with seasonality, where as in other models the drift and diffusion volatility typically do not depend on time. A further advantage of our model is its tractability for pricing derivatives.

By calibrating to two major electricity markets in the US, we show that our model is able to capture both the trajectorial and the statistical properties of electricity prices. This together with its tractability can make our model an attractive alternative for electricity modelling in practice. Future research could focus on further improving the realism of the model by introducing stochastic volatility through absolutely continuous time change as discussed in Remark 1 and by exploring the multi-factor extension as outlined in Remark 3.

Acknowledgements

We thank Prof. Ehud Ronn for helpful discussions and suggestions. We are also very grateful to two anonymous referees and the editor whose suggestions helped to improve the quality of the paper. Lingfei Li acknowledges research support from Hong Kong Research Grant Council ECS Grant No. 24200214.

A Exact Simulation for the Time-Changed JCIR Process

The purpose of this section is to provide an exact simulation algorithm which can be used to generate sample paths from the GMAC-JCIR process. Given $X_s^\phi = x$, we want to simulate the r.v. X_t^ϕ $(t > s)$, which consists of three steps.

- Step 1: Calculate $\int_s^t a(u)du$. Draw a value for $L_{\int_s^t a(u)du}$ (see Cont and Tankov (2004), Chapter 7, Example 6.4, for the exact simulation of the Gamma subordinator). We denote the realization by T.

- Step 2: Simulate the r.v. X_T (i.e., the value of the JCIR process at time T) given it starts at x.
  - Simulate N from the Poisson distribution with parameter ϖT. N gives the total number of jumps on the interval $[0, T]$.
  - Simulate N independent r.v., $U_1, \cdots, U_N$, uniformly distributed on the interval $[0, T]$. These variables mark the jump times.
  - Simulate N independent r.v. $J_1, \cdots, J_N$ from the Exponential distribution with mean μ. These variables correspond to the jump sizes.
  - Let Y denote the CIR process and set $U_{N+1} = T$. Simulate Y_{U_1} given $Y_0 = x$. Then for $i = 2, \cdots, N+1$, simulate Y_{U_i} given the value of the CIR process at time U_{i-1} is $Y_{U_{i-1}} + J_{i-1}$ (see Glasserman (2003), Chapter 3.4, for the exact simulation of the CIR process).
- Step 3: Set $X_T = Y_{U_{N+1}}$.

B Proofs

Proof of Proposition 1: It is clear that the additive subordinator we use satisfies condition (a) to (c) in Theorem 3.1 (ii) of Li et al. (2015). Applying that theorem and using (4), we have

$$\begin{aligned}
\mathcal{G}^{\phi} f(x) &= \gamma a(t) \mathcal{G} f(x) + a(t) \int_{(0,\infty)} (\mathcal{P}_\tau f - f) \nu(d\tau) \\
&= \frac{1}{2} \gamma a(t) \sigma^2 x f''(x) + \gamma a(t) \kappa (1-x) f'(x) + \gamma a(t) \frac{\varpi}{\mu} \int_{(0,\infty)} (f(x+y) - f(x)) e^{-\frac{y}{\mu}} dy \\
&\quad + a(t) \int_{(0,\infty)} (\mathcal{P}_\tau f - f) \nu(d\tau) \qquad (21)
\end{aligned}$$

We write the last term as follows.

$$\begin{aligned}
& a(t) \int_{(0,\infty)} (\mathcal{P}_\tau f - f) \nu(d\tau) \\
&= a(t) \int_{(0,\infty)} \left(\int_{y \neq 0} p(\tau, x, x+y) f(x+y) dy - f(x) \right) \nu(d\tau) \\
&= a(t) \int_{(0,\infty)} \Big(\int_{y \neq 0} p(\tau, x, x+y) [(f(x+y) - f(x) - 1_{\{|y| \leq 1\}} y f'(x)) + f(x) + 1_{\{|y| \leq 1\}} y f'(x)] dy \\
&\quad - f(x) \Big) \nu(d\tau) \\
&= a(t) \int_{y \neq 0} \left(f(x+y) - f(x) - 1_{\{|y| \leq 1\}} y f'(x) \right) \left(\int_{(0,\infty)} p(\tau, x, x+y) \nu(d\tau) \right) dy \qquad (22) \\
&\quad + a(t) f(x) \int_{(0,\infty)} \left(1 - \int_{y \neq 0} p(\tau, x, x+y) dy \right) \nu(d\tau) \\
&\quad + a(t) f'(x) \left(\int_{\{|y| \leq 1\}} y p(\tau, x, x+y) dy \right) \nu(d\tau).
\end{aligned}$$

In the second term, $1-\int_{y\neq 0}p(\tau,x,x+y)dy=0$. Combining the above expression with the third term in Eq.(21), we have

$$
\begin{aligned}
&a(t)\int_{y\neq 0}(f(x+y)-f(x)-1_{\{|y|\leq 1\}}yf'(x))\left(\int_{(0,\infty)}p(\tau,x,x+y)\nu(d\tau)\right)dy\\
&+a(t)f'(x)\left(\int_{\{|y|\leq 1\}}yp(\tau,x,x+y)dy\right)\nu(d\tau)+\gamma a(t)\frac{\varpi}{\mu}\int_{(0,\infty)}(f(x+y)-f(x))e^{-\frac{y}{\mu}}dy\\
&=\int_{y\neq 0}(f(x+y)-f(x)-1_{\{|y|\leq 1\}}yf'(x))\left(\gamma a(t)\frac{\varpi}{\mu}e^{-\frac{y}{\mu}}1_{\{y>0\}}+a(t)\int_{(0,\infty)}p(\tau,x,x+y)\nu(d\tau)\right)dy\\
&+\int_{y\neq 0}1_{\{|y|\leq 1\}}yf'(x)\gamma a(t)\frac{\varpi}{\mu}e^{-\frac{y}{\mu}}1_{\{y>0\}}dy+f'(x)a(t)\left(\int_{\{|y|\leq 1\}}yp(\tau,x,x+y)dy\right)\nu(d\tau)\\
&=\int_{y\neq 0}(f(x+y)-f(x)-1_{\{|y|\leq 1\}}yf'(x))\left(\gamma a(t)\frac{\varpi}{\mu}e^{-\frac{y}{\mu}}1_{\{y>0\}}+a(t)\int_{(0,\infty)}p(\tau,x,x+y)\nu(d\tau)\right)dy\\
&+f'(x)\gamma a(t)\varpi(1-e^{-\frac{1}{\mu}})+f'(x)a(t)\left(\int_{\{|y|\leq 1\}}yp(\tau,x,x+y)dy\right)\nu(d\tau).
\end{aligned}
$$

Combining these equations yields the conclusion. In Eq.(22), we interchanged the order of integration, which we will justify below in two steps.
Step 1: We first show that for the JCIR process, $p(\tau,x,x+y)$ satisfies the following for fixed x.

$$\lim_{\tau\to 0}\frac{\int_{|y|>1}p(\tau,x,x+y)dy}{\tau}=\varpi\int_{|y|>1}\frac{1}{\mu}e^{-\frac{y}{\mu}}dy \tag{23}$$

$$\lim_{\tau\to 0}\frac{\int_{|y|\leq 1}yp(\tau,x,x+y)dy}{\tau}=\kappa(1-x)+\varpi\int_{|y|\leq 1}\frac{y}{\mu}e^{-\frac{y}{\mu}}dy \tag{24}$$

$$\lim_{\tau\to 0}\frac{\int_{|y|\leq 1}y^2p(\tau,x,x+y)dy}{\tau}=\sigma^2x+\varpi\int_{|y|\leq 1}\frac{y^2}{\mu}e^{-\frac{y}{\mu}}dy \tag{25}$$

Let $\overline{p}(\tau;x,x+y)$ be the transition density of the CIR process with the same parameters as in the diffusion part of the JCIR process. Then $\overline{p}(\tau,x,x+y)$ satisfy (23), (24) and (25) with $\varpi=0$ (see Li et al. (2015) Eq.(4.2) to (4.4)). Applying the results in Yu (2007), $p(\tau,x,x+y)$ can be expanded as follows.

$$p(\tau,x,x+y)=\tau^{-\frac{1}{2}}\exp\left(-\frac{C^{(-1)}(x,x+y)}{\tau}\right)\left(C^{(0)}(x,x+y)+C^{(1)}(x,x+y)\tau\right)+D^{(1)}(x,x+y)\tau+o(\tau), \tag{26}$$

with

$$C^{(-1)}(x,x+y)=\frac{1}{2}\left(\int_x^{x+y}\frac{1}{\sigma\sqrt{s}}ds\right)^2=\frac{2}{\sigma^2}\left(\sqrt{x+y}-\sqrt{x}\right)^2,$$

$$C^{(0)}(x,x+y)=\frac{1}{\sqrt{2\pi\sigma^2(x+y)}}\left(\frac{x+y}{x}\right)^{-\frac{1}{4}+\frac{\kappa}{\sigma^2}}\exp\left(-\frac{\kappa y}{\sigma^2}\right),$$
$$D^{(1)}(x,x+y)=\frac{\omega}{\mu}e^{-\frac{1}{\mu}y}.$$

The coefficient $C^{(1)}$ is can be calculated recursively from and $C^{(-1)}$ and $C^{(0)}$ as explained in Yu (2007), nonetheless the explicit expression of such coefficient will not be needed in our proof. Again from Yu (2007), for the CIR process,

$$\overline{p}(\tau,x,x+y)=\tau^{-\frac{1}{2}}\exp\left(-\frac{C^{(-1)}(x,x+y)}{\tau}\right)\left(C^{(0)}(x,x+y)+\overline{C}^{(1)}(x,x+y)\tau\right)+o(\tau),$$

with the same $C^{(-1)}(x,x+y)$ and $C^{(0)}(x,x+y)$ as the JCIR process. For $\overline{C}^{(1)}$, again we do not need its explicit expression. Hence

$$\begin{aligned}
&\lim_{\tau\to0}\frac{\int_{|y|>1}p(\tau,x,x+y)dy}{\tau}-\lim_{\tau\to0}\frac{\int_{|y|>1}\overline{p}(\tau,x,x+y)dy}{\tau}\\
&=\lim_{\tau\to0}\int_{|y|>1}\tau^{-\frac{1}{2}}\exp\left(-\frac{C^{(-1)}(x,x+y)}{\tau}\right)(C^{(1)}(x,x+y)-\overline{C}^{(1)}(x,x+y))dy+\int_{|y|>1}D^{(1)}(x,x+y)dy\\
&=\varpi\int_{|y|>1}\frac{1}{\mu}e^{-\frac{y}{\mu}}dy,
\end{aligned}$$

which shows (23). Eqs. (24) and (25) can be proved similarly.
Step 2: For $f\in C_c^2(I)$, it is easy to see $|f(x+y)-f(x)-1_{\{|y|\le1\}}yf'(x)|\le C_x(1\wedge y^2)$ for some positive constant C_x. If we can show

$$\int_{(0,\infty)}\int_{y\neq0}(1\wedge y^2)p(\tau,x,x+y)dy\nu(d\tau)<\infty,$$

then the dominated convergence theorem can be applied to justify the interchange. This result also implies that $\Pi^\phi(t,x,dy)$ is a Lévy-type measure. Eqs. (23) and (25) imply that $\int_{|y|\le1}y^2p(\tau,x,x+y)dy+\int_{|y|>1}p(\tau,x,x+y)dy\sim O(\tau)$ as $\tau\to0$. Also, we know that $\int_{(0,\infty)}(\tau\wedge1)\nu(d\tau)<\infty$. So, we can conclude $\int_{(0,\infty)}\int_{y\neq0}(1\wedge y^2)p(\tau,x,x+y)dy\nu(d\tau)<\infty$. Similarly, we can conclude that the term $\int_{(0,\infty)}(\int_{\{|y|\le1\}}yp(\tau,x,x+y)dy)\nu(d\tau)<\infty$ since $\int_{\{|y|\le1\}}yp(\tau,x,x+y)dy\sim O(\tau)$ as $\tau\to0$ by (24). This concludes the proof. □

Proof of Proposition 2: Note that

$$\frac{\int_{|y|>1}p(\tau,x,x+y)dy}{\tau},\ \frac{\int_{|y|\le1}yp(\tau,x,x+y)dy}{\tau},\ \frac{\int_{|y|\le1}y^2p(\tau,x,x+y)dy}{\tau}\tag{27}$$

are jointly continuous in (τ,x) for $\tau>0$ and $x>0$. Since the right-hand-side in (23), (24) and (25) is continuous in x, it is not difficult to see that for any compact set K for x, the three quantities in (27) are bounded on $[0,1]\times K$. For $\tau>1$, notice that $\int_{|y|>1}p(\tau,x,x+y)dy$ and $\int_{|y|\le1}yp(\tau,x,x+y)dy$ are bounded by 1. Therefore, for $x\in K$,

$$\left|\int_{(0,\infty)}\left(\int_{\{|y|\le1\}}yp(\tau,x,x+y)dy\right)\nu(t,d\tau)\right|\le C_1a(t)\int_{(0,\infty)}(\tau\wedge1)\nu(d\tau),$$

$$\left|\int_{y\neq 0}(y^2\wedge 1)\widehat{\Pi}^{\psi}(t,x,dy)\right|\leq C_2 a(t)\int_{(0,\infty)}(\tau\wedge 1)\nu(d\tau).$$

for some positive constant C_1, C_2 which do not depend on t and x. Furthermore, since $a(t)$ is continuous, on any compact set for t, $a(t)\int_{(0,\infty)}(\tau\wedge 1)\nu(d\tau)$ is bounded. This implies that

$$\mu^{\phi}(t,x),\sigma^{\phi}(t,x) \text{ and } \int_{y\neq 0}(y^2\wedge 1)\widehat{\Pi}^{\phi}(t,x,dy)$$

are bounded on every compact set for t and x. To show X^{ϕ} is a semimartingale with characteristics triplet $(B^{\phi},C^{\phi},\nu^{\phi})$ w.r.t. the truncation function $h(x)=x1_{\{|x|\leq 1\}}$, one can then follow the arguments in the proof of Proposition 3.2 in Cheridito et al. (2005). The sample path decomposition is a result of Theorem II.2.34 in Jacod and Shiryaev (2003). □

Proof of Lemma 1: Let $A_t^{-1}:=\inf\{s\geq 0: A_s=t\}$, be the inverse of $A_t=\int_0^t a(u)du$. Since $a(u)>0$, the inverse is also increasing. Note that $A_t^{-1}=\int_0^t\frac{1}{a(u)}du$. Define $X_t^{\psi}:=X^{\phi}_{A_t^{-1}}$. It is easy to see that $X_t^{\psi}=X_{L_t}$. Consider a probability measure $\overline{\mathbb{P}}$ on $(\Omega,(\mathcal{F}_t)_{t\geq 0})$, such that X^{ϕ} is a semimartingale with characteristics $(B^{\overline{\phi}},C^{\overline{\phi}},\nu^{\overline{\phi}})$. From Corollary 10.12 in Jacod (1979), X^{ψ} is also a semimartingale on $(\Omega,(\mathcal{F}_t)_{t\geq 0})$ with characteristics $(B^{\overline{\psi}},C^{\overline{\psi}},\nu^{\overline{\psi}})$ w.r.t. to the truncation function $h(x)=x1_{\{|x|\leq 1\}}$, where

$$\begin{aligned}
B_t^{\overline{\psi}}(\omega)&=\int_0^t\Big[\overline{\gamma}\cdot\overline{\kappa}(1-X_{s-}^{\psi}(\omega))+\overline{\gamma}\cdot\overline{\varpi}\left(1-e^{-\frac{1}{\overline{\mu}}}\right)\\
&+\int_{(0,\infty)}\int_{\{|y|\leq 1\}}y\overline{p}(\tau,X_{s-}^{\psi}(\omega),X_{s-}^{\psi}(\omega)+y)dy\overline{\nu}(d\tau)\Big]ds,\\
C_t^{\overline{\psi}}(\omega)&=\int_0^t\overline{\gamma}\cdot\overline{\sigma}^2X_{s-}^{\psi}(\omega)ds,\\
\nu^{\overline{\psi}}(\omega,dt,dy)&=\left[1_{\{y>0\}}\overline{\gamma}\frac{\overline{\varpi}}{\overline{\mu}}e^{-\frac{y}{\overline{\mu}}}+\pi^{\overline{\psi}}(X_{s-}^{\psi},y)\right]dydt,\ \pi^{\overline{\psi}}(x,y)=\int_{(0,\infty)}\overline{p}(\tau,x,x+y)\overline{\nu}(d\tau).
\end{aligned}$$

Thus a solution to the martingale problem for X^{ϕ} associated with $(B^{\overline{\phi}},C^{\overline{\phi}},\nu^{\overline{\phi}})$ is also a solution to the the martingale problem for X^{ψ} associated with $(B^{\overline{\psi}},C^{\overline{\psi}},\nu^{\overline{\psi}})$. We next show the solution to the latter problem is unique, and hence so is the solution to the former problem.

We first find out the infinitesimal generator of X^{ψ}, denoted by $\mathcal{G}^{\psi}$. Note that $X_t^{\psi}=X_{L_t}$. Applying the Phillips Theorem (Sato (1999), Theorem 32.1), and using similar arguments in the proof of Proposition 1, for $f\in C_c^2(I)$,

$$\begin{aligned}
\mathcal{G}^{\psi}f(x)&=\frac{1}{2}\left(\sigma^{\overline{\psi}}(x)\right)^2f''(x)+\mu^{\overline{\psi}}(x)f'(x)\\
&+\int_{y\neq 0}(f(x+y)-f(x)-1_{\{|y|\leq 1\}}yf'(x))\left(1_{\{y>0\}}\overline{\gamma}\frac{\overline{\varpi}}{\overline{\mu}}e^{-\frac{y}{\overline{\mu}}}+\pi^{\overline{\psi}}(x,y)\right)dy
\end{aligned}$$

where

$$\sigma^{\overline{\psi}}(x)=\overline{\sigma}p\sqrt{\overline{\gamma}x},\mu^{\overline{\psi}}(x)=\overline{\gamma}\cdot\overline{\kappa}(1-x)+\overline{\gamma}\cdot\overline{\varpi}\left(1-e^{-\frac{1}{\overline{\mu}}}\right)+\int_{(0,\infty)}\int_{\{|y|\leq 1\}}y\overline{p}(\tau,x,x+y)dy\overline{\nu}(d\tau).$$

Notice that $C_c^2(I)$ is a core for the generator of the JCIR process (Duffie et al. (2003), Theorem 2.7), hence by the Phillips Theorem, it is also a core for the generator of X^ψ.

Let $\overline{\mathbb{P}}$ be a solution to the martingale problem for X^ψ associated with $(B^{\overline{\psi}}, C^{\overline{\psi}}, \nu^{\overline{\psi}})$. We want to show, for $f \in C_c^2(I)$,

$$M_t := f(X_t^\psi) - f(x_0) - \int_0^t \mathcal{G}^\psi f(X_{s-}^\psi) ds$$

is a martingale. This implies a solution to the martingale problem in the sense of Jacod and Shiryaev (2003) is also a solution to the martingale problem in the sense of Ethier and Kurtz (1986). We can then conclude uniqueness of solutions using Theorem 4.1 and Corollary 4.3 in Ethier and Kurtz (1986). Notice that, M_t is a local martingale by Theorem II.2.42(c) of Jacod and Shiryaev (2003). Since $\mathcal{G}^\psi f \in C_0(I)$, $\mathcal{G}^\psi f$ is bounded. $f(X_t^\psi)$ is also bounded for all t. Hence, $\overline{\mathbb{E}}[M_t^*] < \infty$ ($M_t^* := \sup_{s \le t} |M_s|$) for all t. By Protter (2004), Chapter 1, Theorem 51, M_t is a martingale. This concludes the proof. □

Proof of Proposition 3: With Lemma 1, the proof is similar to the proof of Theorem 3.2 in Li and Mendoza-Arriaga (2015), which we refer to for details. □

Proof of Proposition 4: To prove the claim, we will apply Proposition 4.3 and 4.4 in Li and Mendoza-Arriaga (2015). Note that these results can still be applied if the background process is a jump-diffusion although Li and Mendoza-Arriaga (2015) only considers the diffusion case. Define

$$q(\tau, x, x+y) = \frac{1}{\sqrt{2\pi\sigma^2\tau(x+y)}} \left(\frac{x+y}{x}\right)^{-1/4+\kappa\theta/\sigma^2} \exp\left(-\frac{2(\sqrt{x+y}-\sqrt{x})^2}{\sigma^2\tau} - \frac{\kappa y}{\sigma^2}\right).$$

Using (26) and that the JCIR process is a stationary process with a continuous stationary density, it is not difficult to check that $q(\tau, x, x+y)$ satisfies Assumption 4.1 and 4.2 in Li and Mendoza-Arriaga (2015). We next calculate the asymptotics of $a(s)\int_{[0,\Delta)} q(\tau, x, x+y)\nu(d\tau)$ as $y \to 0$ for some $\Delta \in (0,1)$. Define

$$f(x,y) := (x+y)^{-\frac{1}{2}} \left(\frac{x+y}{x}\right)^{-1/4+\kappa\theta/\sigma^2} \exp\left(-\frac{\kappa y}{\sigma^2}\right), \; g(s) := Ca(s).$$

Let $u = 2(\sqrt{x+y}-\sqrt{x})^2/(\sigma^2\tau)$. Then we have

$$\begin{aligned}
&a(s)\int_{[0,\Delta)} q(\tau, x, x+y)\nu(d\tau) \\
&= a(s)f(x,y)\frac{|\sqrt{x+y}-\sqrt{x}|}{\sigma^2\sqrt{\pi}} \int_{\frac{2(\sqrt{x+y}-\sqrt{x})^2}{\sigma^2\Delta}}^\infty u^{-\frac{3}{2}} e^{-u} \nu\left(\frac{2(\sqrt{x+y}-\sqrt{x})^2}{\sigma^2 u}\right) du \\
&= f(x,y)g(s)\frac{\sigma^{2p}}{2^{p+1}\sqrt{\pi}} \left|\sqrt{x+y}-\sqrt{x}\right|^{-2p-1} \int_{\frac{2(\sqrt{x+y}-\sqrt{x})^2}{\sigma^2\Delta}}^\infty u^{p-\frac{1}{2}} e^{-u} \exp\left(-\eta\frac{2(\sqrt{x+y}-\sqrt{x})^2}{\sigma^2 u}\right) du \\
&\sim g(s)\frac{\sigma^{2p}\Gamma(p+\frac{1}{2})}{2^{p+1}\sqrt{\pi x}} \left|\sqrt{x+y}-\sqrt{x}\right|^{-2p-1} \text{ as } y \to 0,
\end{aligned}$$

where $\Gamma(\cdot)$ is the Gamma function. Proposition 4.4 in Li and Mendoza-Arriaga (2015) implies that

$$p = \overline{p}, \; Ca(s)\frac{\sigma^{2p}\Gamma(p+\frac{1}{2})}{2^{p+1}\sqrt{\pi}} = \overline{C}\overline{a}(s)\frac{\overline{\sigma}^{2\overline{p}}\Gamma(\overline{p}+\frac{1}{2})}{2^{\overline{p}+1}\sqrt{\pi}}. \tag{28}$$

Proposition 4.3 in Li and Mendoza-Arriaga (2015) shows that (28) is also sufficient for Condition (ii) in Proposition 3 to hold. Clearly (28) is equivalent to $p = \overline{p}$, $Ca(s)\sigma^{2p} = \overline{C}\overline{a}(s)\overline{\sigma}^{2p}$. This completes the proof. □

Proof of Proposition 5: We first calculate $\mathbb{E}_x[X_t]$ and $\mathbb{E}_{s,x}[X_t^\phi]$. Since under $\overline{\mathbb{P}}$, X^ϕ remains as a LAC-JCIR process, the result under $\overline{\mathbb{P}}$ is obtained by using parameters with an overhead bar. Recall that the Laplace transform of the JCIR process is given by (11). Note that

$$\mathbb{E}_x[X_t] = -\frac{\partial \mathbb{E}_x[e^{-\lambda X_t}]}{\partial \lambda}\Big|_{\lambda=0}.$$

The first order derivative of the Laplace transform can be calculated directly. Note that,

$$\begin{aligned}
&\frac{\partial A(\lambda;t)}{\partial \lambda}\Big|_{\lambda=0} = e^{-\kappa t} - 1, \quad \frac{\partial B(\lambda;t)}{\partial \lambda}\Big|_{\lambda=0} = e^{-\kappa t}, \\
&\frac{\partial C(\lambda;t)}{\partial \lambda}\Big|_{\lambda=0} = -\varpi a e^{-\kappa t}(e^{-\kappa t} - 1)\left(\frac{\sigma^2}{2\kappa} - \mu\right).
\end{aligned}$$

Hence,

$$\begin{aligned}
\frac{\partial \mathbb{E}_x[e^{-\lambda X_t}]}{\partial \lambda}\Big|_{\lambda=0} &= \Big[\frac{\partial A(\lambda;t)}{\partial \lambda} C(\varpi,\lambda;t) e^{-B(\lambda;t)x} + \frac{\partial C(\varpi,\lambda;t)}{\partial \lambda} A(\lambda;t) e^{-B(\lambda;t)x} \\
&\quad + A(\lambda;t)C(\lambda;t)(-x)e^{-B(\lambda;t)x}\frac{\partial B(\lambda;t)}{\partial \lambda}\Big]\Big|_{\lambda=0} \\
&= e^{-\kappa t}(1 - x + \frac{\mu\varpi}{\kappa}) - (1 + \frac{\mu\varpi}{\kappa})
\end{aligned}$$

Thus

$$\mathbb{E}_x[X_t] = -e^{-\kappa t}(1 - x + \frac{\mu\varpi}{\kappa}) + (1 + \frac{\mu\varpi}{\kappa}).$$

For the LAC-JCIR process,

$$\begin{aligned}
\mathbb{E}_{s,x}[X_t^\phi] &= \int_{[0,\infty)} \mathbb{E}_x[X_u] q_{s,t}(du) = \int_{[0,\infty)} \left[-e^{-\kappa u}(1 - x + \frac{\mu\varpi}{\kappa}) + (1 + \frac{\mu\varpi}{\kappa})\right] q_{s,t}(du) \\
&= -e^{-\psi(\kappa)\int_s^t a(u)du}(1 - x + \frac{\mu\varpi}{\kappa}) + (1 + \frac{\mu\varpi}{\kappa})
\end{aligned} \tag{29}$$

For the futures price, using (29),

$$\begin{aligned}
F(t,T_1,T_2) &= \frac{1}{M}\overline{\mathbb{E}}\left[\sum_{i=0}^{M} S_{T_1+ih}\Big|\mathcal{F}_t\right] = \frac{1}{M}\overline{\mathbb{E}}\left[\sum_{i=0}^{M} S_{T_1+ih}\Big|X_t^\phi\right] \\
&= \frac{1}{M}\sum_{i=0}^{M}\overline{\mathbb{E}}\left[\Lambda(T_1+ih)X^\phi_{T_1+ih}\Big|X_t^\phi\right] = A(t,T_1,T_2)X_t^\phi + B(t,T_1,T_2).
\end{aligned}$$

This concludes the proof. □

Proof of Proposition 6: If $K \le B(T,T_1,T_2)$, from (19), the put price is obviously zero. If $K > B(T,T_1,T_2)$, given $X_t^\phi = x$,

$$P(k,t,T,T_1,T_2) = e^{-r(T-t)}A(T,T_1,T_2)\overline{\mathbb{E}}\left[(k - X_T^\phi)1_{\{X_T^\phi<k\}}\Big|X_t^\phi = x\right]$$

$$= e^{-r(T-t)} A(T, T_1, T_2) \int_0^k (k-y) p^{\overline{\phi}}(t, T, x, y) dy,$$

where $p^{\overline{\phi}}(t, T, x, y)$ is the transition probability density of X^{ϕ}. Clearly the above integral is the convolution of two functions: $f(y) = y$ and $p^{\overline{\phi}}(t, T, x, y)$. Hence its Laplace transform is the product of the Laplace transform of each function. The Laplace transform of f is $1/\lambda^2$. Therefore

$$L_P(\lambda) = e^{-r(T-t)} A(T, T_1, T_2) \frac{1}{\lambda^2} \overline{\mathbb{E}}_{t,x} \left[e^{-\lambda X_T^{\phi}} \right].$$

This concludes the proof. □

Proof of Proposition 7: This can be directly verified from Eq.(13), the transition density of the Gamma subordinator and Eq.(14). □

References

Abate, J. and W. Whitt (1992). The Fourier-series method for inverting transforms of probability distributions. *Queueing systems 10*(1-2), 5–87.

Albanese, C., H. Lo, and S. Tompaidis (2012). A numerical method for pricing electricity derivatives based on continuous time lattices. *European Journal of Operational Research 222*, 361–368.

Barndorff-Nielsen, O. E. (1998). Processes of Normal Inverse Gaussian type. *Finance and Stochastics 2*, 41–68.

Barndorff-Nielsen, O. E. and S. Levendorskiĭ (2001). Feller processes of Normal Inverse Guassian type. *Quantitative Finance 1*, 318–331.

Benth, F. E., J. Kallsen, and T. Meyer-Brandis (2007). A Non-Gaussian Ornstein–Uhlenbeck process for electricity spot price modeling and derivatives pricing. *Applied Mathematical Finance 14*(2), 153–169.

Benth, F. E., R. Kiesel, and A. Nazarova (2012). A critical empirical study of three electricity spot price models. *Energy Economics 34*, 1589–1616.

Benth, F. E., J. Šaltytė Benth, and S. Koekebakker (2008). *Stochastic Modelling of Electricity and Related Markets*. Singapore: World Scientific.

Billingsley, P. (1961). *Statistical Inferences for Markov Processes*. Chicago: The University of Chicago Press.

Birge, J., N. Cai, and S. Kou (2010). A two-factor model for electricity spot and futures prices. Working Paper.

Boyarchenko, N. and S. Z. Levendorskiĭ (2007). The eigenfunction expansion method in multifactor quadratic term structure models. *Mathematical Finance 17*(4), 503–539.

Boyarchenko, S. I. and S. Levendorskiĭ (2002). *Non-Gaussian Merton-Black-Scholes Theory*, Volume 9. World Scientific.

Burger, M., B. Klar, A. Müller, and G. Schindlmayr (2004). A spot market model for pricing derivatives in electricity markets. *Quantitative Finance 4*(1), 109–122.

Carr, P., H. Geman, D. B. Madan, and M. Yor (2002). The fine structure of asset returns: an empirical investigation. *Journal of Business 75*(2), 305–332.

Cartea, A. and M. G. Figueroa (2005). Pricing in electricity markets: A mean reverting jump diffusion model with seasonality. *Applied Mathematical Finance 12*(4), 313–335.

Cartea, A. and P. Villaplana (2008). Spot price modeling and the valuation of electricity forward contracts: the role of demand and capacity. *Journal of Banking & Finance 32*(12), 2502–2519.

Cheridito, P., D. Filipović, and M. Yor (2005). Equivalent and absolutely continuous measure change for jump-diffusion processes. *The Annals of Applied Probability 15*(3), 1713–1732.

Cont, R. and P. Tankov (2004). *Financial Modeling with Jump Processes*. Cambridge: Chapman & Hall.

Deng, S. J. (1999). Stochastic models of energy commodity prices and their applications: mean reversion with jumps and spikes. Technical report, POWER.

Diebold, F. X. and R. S. Mariano (1995). Comparing predictive accuracy. *Journal of Business & Economic Statistics 16*(4), 134–144.

Duffie, D., D. Filipović, and W. Schachermayer (2003). Affine processes and application in finance. *The Annals of Applied Probability 13*(3), 984–1053.

Duffie, D. and N. Gârleanu (2001). Risk and valuation of collaterized debt obligations. *Financial Analysts Journal 57*(1), 41–59.

Escribano, A., J. I. Peña, and P. Villaplana (2011). Modelling electricity prices: International evidence. *Oxford Bulletin of Economics and Statistics 73*(5), 622–650.

Ethier, S. N. and T. G. Kurtz (1986). *Markov Processes: Characterization and Convergence*. Hoboken: John Wiley & Sons, Inc.

Eydeland, A. and K. Wolyniec (2003). *Energy and Power Risk Management*. Hoboken: John Wiley & Sons Inc.

Fang, F. and C. W. Oosterlee (2009). Pricing early-exercise and discrete barrier options by Fourier-cosine series expansions. *Numerische Mathematik 114*(1), 27–62.

Geman, H. (2005). *Commodities and Commodity Derivatives: Modeling and Pricing for Agriculturals, Metals and Energy*. Hoboken: John Wiley & Sons Inc.

Geman, H. and S. Kourouvakalis (2008). A lattice-based method for pricing electricity derivatives under the threshold model. *Applied Mathematical Finance 15*(6), 531–567.

Geman, H. and A. Roncoroni (2006). Understanding the fine structure of electricity prices. *The Journal of Business 79*(3), 1225–1261.

Glasserman, P. (2003). *Monte Carlo Methods in Financial Engineering*. New York: Springer.

Gulisashvili, A. and J. A. Van Casteren (2006). *Non-Autonomous Kato Classes and Feynman-Kac Propagators*. Singapore: World Scientific.

Hambly, B., S. Howison, and T. Kluge (2009). Modeling spikes and pricing swing options in electricity markets. *Quantitative Finance 9*(8), 937–949.

Hayfavi, A. and I. Talasli (2014). Stochastic multifactor modeling of spot electricity prices. *Journal of Computational and Applied Mathematics 259*, 434–442.

Huisman, R. and R. Mahieu (2001). Regime jumps in electricity prices. *Energy Economics 25*(5), 425–434.

Jacod, J. (1979). Calcul stochastique et problèmes de martingales. In *Lecture Notes in Mathematics*, Volume 714. Berlin: Springer.

Jacod, J. and A. Shiryaev (2003). *Limit Theorems for Stochastic Processes*. Berlin: Springer.

Jaimungal, S. and V. Surkov (2011). Lévy-based cross-commodity models and derivative valuation. *SIAM Journal on Financial Mathematics 2*(1), 464–487.

Kjaer, M. (2008). Pricing of swing options in a mean-reverting model with jumps. *Applied Mathematical Finance 15*(5), 479–502.

Klüppelberg, C., T. Meyer-Brandis, and A. Schmidt (2010). Electricity spot price modelling with

a view towards extreme spike risk. *Quantitative Finance 10*(9), 963–974.

Li, J., L. Li, and R. Mendoza-Arriaga (2015). Additive subordination and its applications in finance. Preprint.

Li, L. and V. Linetsky (2014). Time-changed Ornstein-Uhlenbeck processes and their applications in commodity derivative models. *Mathematical Finance 24*(2), 289–330.

Li, L. and R. Mendoza-Arriaga (2015). Equivalent measure changes for subordinate diffusions. Preprint.

Lim, D., L. Li, and V. Linetsky (2012). Evaluating Callable and Putable Bonds: An Eigenfunction Expansion Approach. *Journal of Economic Dynamics and Control 36*(12), 1888–1908.

Lucia, J. J. and E. S. Schwartz (2002). Electricity prices and power derivatives: evidence from the nordic power exchange. *Review of Derivatives Research 5*(1), 5–50.

Madan, D., P. Carr, and E. C. Chang (1998). The Variance Gamma process and option pricing. *European Finance Review 2*, 79–105.

Madan, D. and M. Yor (2008). Representing the CGMY and Meixner Lévy processes as time changed Brownian motions. *Journal of Computational Finance 12*(1), 27–47.

Mendoza-Arriaga, R., P. Carr, and V. Linetsky (2010). Time changed Markov processes in unified credit-equity modeling. *Mathematical Finance 20*(4), 527–569.

Mendoza-Arriaga, R. and V. Linetsky (2013). Time-changed CIR default intensities with two-sided mean-reverting jumps. To appear in *The Annals of Applied Probability*.

Meyer-Brandis, T. and P. Tankov (2008). Multi-factor jump-diffusion models of electricity prices. *International Journal of Theoretical and Applied Finance 11*(5), 503–528.

Nomikos, N. K. and O. Soldatos (2008). Using affine jump diffusion models for modelling and pricing electricity derivatives. *Applied Mathematical Finance 15*(1), 41–71.

Press, W. H., S. A. Teukolsky, W. T. Vetterling, and B. P. Flannery (1996). *Numerical Recipes in C* (2nd ed.). Cambridge: Cambridge University Press.

Protter, P. (2004). *Stochastic Integration and Differential Equations*. Berlin: Springer.

Sato, K. (1999). *Lévy Processes and Infinitely Divisible Distributions*. Cambridge: The Cambridge University Press.

Schwartz, E. S. (1997). The stochastic behavior of commodity prices: Implications for valuation and hedging. *The Journal of Finance 52*(3), 923–973.

Singleton, K. (2001). Estimation of affine asset pricing models using the empirical characteristic function. *Journal of Econometrics 102*, 111–141.

Song, R. and Z. Vondraček (2008). On the relationship between subordinate killed and killed subordinate processes. *Electronic Communications in Probability 13*, 325–336.

Veraart, A. E. and L. A. Veraart (2014). Modelling electricity day-ahead prices by multivariate Lévy semistationary processes. In *Quantitative Energy Finance*, pp. 157–188. Springer.

Weron, R. (2008). Market price of risk implied by Asian-style electricity options and futures. *Energy Economics 30*(3), 1098–1115.

Weron, R., M. Bierbrauer, and S. Trück (2004). Modelling electricity prices: jump diffusion and regime switching. *Physica A 336*, 39–48.

Yu, J. (2007). Closed-form likelihood approximation and estimation of jump-diffusions with an application to the realignment risk of the Chinese Yuan. *Journal of Econometrics 141*(2), 1245–1280.

Zhang, B. and C. Oosterlee (2013). An efficient pricing algorithm for swing options based on Fourier cosine expansions. *Journal of Computational Finance 16*(4), 1–32.